

Modelling and control of manipulators for inspection and maintenance in challenging environments: A literature review

Alessandro Pistone^{a,*}, Daniele Ludovico^a, Lorenzo De Mari Casareto Dal Verme^{b,a}, Sergio Leggieri^a, Carlo Canali^a, Darwin G. Caldwell^a

^a Advanced Robotics (ADVR), Istituto Italiano di Tecnologia, Via Morego, 30, Genova, 16163, Italy

^b Dipartimento di Informatica, Bioingegneria, Robotica e Ingegneria dei Sistemi (DIBRIS), Università di Genova, Via Balbi, 5, Genova, 16126, Italy

ARTICLE INFO

Keywords:

Manipulators
Mobile manipulators
Inspection and maintenance
Modelling
Control
Challenging environments

ABSTRACT

Nowadays, the use of robotic systems for inspection and maintenance is gaining importance due to the number of scenarios in which robots can operate. Indeed, robotic systems provide many advantages in harsh and hostile environments, improving workers' safety and overall efficiency. Given their ability to perform different tasks, robotic manipulators constitute a significant proportion of the possible robotic systems employed in these environments. The category of manipulators is a heterogeneous group that comprises many different types of robots: non-redundant, redundant, and hyper-redundant manipulators, the latter being subdivided into discrete-joint manipulators and continuum manipulators. Among these types of robots, hyper-redundant manipulators play a crucial role in operating in challenging environments due to their ability to perform auxiliary tasks, such as obstacle avoidance and joint limits satisfaction. Furthermore, manipulators can be made of rigid or soft mechanisms and can be mobile, operating in aerial, ground, and underwater environments. The objective of this review article is to provide a reference point for researchers interested in modelling and controlling manipulators for inspection and maintenance in challenging environments.

1. Introduction

In many fields of human activity, there is a need to perform tasks in dangerous environments that could seriously compromise the health of the people involved in such operations. In this context, remotely performing inspection and maintenance tasks using robotic systems could improve workers' safety and overall efficiency. At the same time, challenging environments for inspection and maintenance robots comprise conditions with obstacles, hazards, or complexities that impede effective robot operation. These may include confined spaces, uneven terrain, extreme temperatures, high-pressure areas, radioactive environments, and even void space. Thus, inspection and maintenance robots designed for challenging environments are often equipped with specialised features, sensors, and capabilities to navigate, assess, and address issues in these difficult conditions, ensuring the safe and efficient execution of inspection and maintenance tasks. Ultimately, from the mechanical, electrical, and control points of view, their design is also driven by the environments in which they need to operate. In recent years, a variety of devices have been developed to accomplish inspection and maintenance tasks in challenging environments: wheeled and crawler robots, legged robots, aerial and underwater

mobile robots, and manipulators. For inspection and maintenance in harsh and hazardous environments, robotic manipulators constitute a significant proportion of the possible choices. Within this type of robot, hyper-redundant manipulators have been implemented in many fields of application, such as the nuclear sector, medicine, industrial facilities, and even aerospace environments because they can move through hazardous and harsh environments due to their redundancy. In fact, a robotic manipulator is considered redundant with respect to a specific task if it has more Degrees of Freedom (DoF) than the minimum number of DoF required to perform the task. If the extra DoF are two or more, the manipulator is considered hyper-redundant with respect to the task. The large number of DoF that characterise the kinematic redundancy allows the robot to perform multiple tasks simultaneously, like moving into constrained environments on a specific trajectory while avoiding possible obstacles. Conversely, the complexity of these robots, which can comprise discrete-joint manipulators, in which each of the DoF is driven by at least one motor, or continuum manipulators, in which the number of joints tends to infinity and the links length tends to zero, increases the modelling and control challenges. Besides hyper-redundant manipulators, another solution to inspect and operate in

* Corresponding author.

E-mail addresses: alessandro.pistone@iit.it (A. Pistone), daniele.ludovico@iit.it (D. Ludovico), lorenzo.demarcasareto@iit.it (Lorenzo De Mari Casareto Dal Verme), sergio.leggieri@iit.it (S. Leggieri), carlo.canali@iit.it (C. Canali), darwin.caldwell@iit.it (D.G. Caldwell).

<https://doi.org/10.1016/j.arcontrol.2024.100949>

Received 11 July 2023; Accepted 6 March 2024

Available online 16 March 2024

1367-5788/© 2024 The Author(s). Published by Elsevier Ltd. This is an open access article under the CC BY-NC-ND license (<http://creativecommons.org/licenses/by-nc-nd/4.0/>).

List of important acronyms

DoF	Degrees of Freedom
DJHRM	Discrete-Joint Hyper-Redundant Manipulator
UAVs	Unmanned Aerial Vehicles
AUVs	Autonomous Underwater Vehicles
ROVs	Remotely Operated Vehicles
DH	Denavit–Hartenberg
ANN	Artificial Neural Network
BPNN	Back Propagation Neural Network
CNN	Convolutional Neural Network
FEA	Finite Element Analysis
EMG	ElectroMyoGraphy
GUI	Graphical User Interface
HRI	Human–Robot Interaction
IMU	Inertial Measurement Unit
RH	Remote Handling

challenging environments are mobile manipulators, which consist of manipulators mounted on mobile platforms that can be autonomous or teleoperated. Unlike fixed-based manipulators, mobile manipulators can navigate in broad areas, and therefore, they are particularly suitable for large industrial sites or even outdoors. In this context, a systematic literature review was performed focusing on modelling and control of manipulators for inspection and maintenance in hazardous environments.

The article is structured as follows. Section 2 presents the research methodology to comprehensively identify documents on modelling and control of manipulators for inspection and maintenance in challenging environments. Section 3 details the literature review of discrete-joint hyper-redundant manipulators, Section 4 focuses on continuum manipulators, and Section 5 considers mobile manipulators. Section 6 summarises the information found on the remaining types of manipulators. Finally, Section 7 discusses the results.

2. Research procedure

For this work, two different queries were performed on the Scopus database. Only Scopus was used as a database since, as proven by Giustini and Boulos (2013), Delgado López-Cózar, Orduña-Malea, and Martín-Martín (2019), Martín-Martín, Thelwall, Orduña-Malea, and Delgado López-Cózar (2021), and Singh, Singh, Karmakar, Leta, and Mayr (2021), it extensively covers documents and sources while supporting different search operators, allowing to carry out a complete, accurate, and reproducible systematic literature review. Only documents written in English were selected. In addition, all the documents published before 2018 without at least one citation were removed. The first query was designed to find documents focusing on modelling and controlling generic robots for inspection and maintenance in challenging environments, without restricting to a particular robot category. The results led to defining a second query focused on the most common type of robot for these tasks, i.e. manipulators. This section describes the research procedure employed for this work.

2.1. Queries description

The string corresponding to the first query is reported in Section 2.2. In June 2023, this query retrieved 408 unique documents. A selection was applied to remove documents that were impossible to obtain, and others considered “out of scope” because they did not fit the original search, i.e. such documents did not focus on modelling and controlling generic robots for inspection and maintenance in challenging environments. Fig. 1 reports a schematic of the research procedure for the first query, where the Scopus queries syntax is defined as follows:

TITLE-ABS-KEY	search the specified terms within document title, abstract, and keywords;
AND	only documents that contain all of the terms linked by this operator are found;
OR	all the documents that contain any of the terms linked by this operator are found;
PRE/2	the first term in the query must precede the second by two or fewer words.

The 294 valid documents selected were classified according to the robot type: manipulators (~ 32 %), mobile grounded robots (~ 28 %), mobile aerial robots (~ 16 %), mobile underwater robots (~ 7 %), and robotic systems (~ 6 %). The remaining ~ 10 % contains types of robot which appear with a frequency not statistically relevant, i.e. $\lesssim 1$ %. Since manipulators are the main robot type resulting from this first query, a second query was performed to obtain a more homogeneous review and isolate documents on modelling and control of manipulators for inspection and maintenance in challenging environments. The string corresponding to this second query is reported in Section 2.2. In June 2023, this query retrieved 119 different documents. Subsequently to the editorial review process, in January 2024 this query retrieved 126 different documents. Again, a filter was applied to remove documents that were impossible to obtain or “out of scope”, i.e. documents not focusing on modelling and controlling manipulators for inspection and maintenance in challenging environments. The resulting sample was enriched by adding the most relevant documents from the collection of documents obtained by looking at the references of the sample itself, a technique known as backward snowballing, and from the collection of documents that cite the sample itself, a technique known as forward snowballing. This gave a total of 121 documents. Fig. 2 reports a schematic of the research procedure for the second query. The robots described by those documents were classified according to the following definitions:

hyper-redundant manipulator a mechanism with many more DoF than are necessary to position and orient its end-effector. There are two possible categories:

discrete-joint manipulator a fully-actuated or over-actuated hyper-redundant manipulator, i.e. each of the DoF is driven by at least one motor;

continuum manipulator a hyper-redundant manipulator with a backbone structure where the number of joints can tend to infinity, but with link lengths tending to zero;

mobile manipulator a manipulator (non-redundant, redundant, or hyper-redundant) connected to a mobile base and able to operate in aerial, ground, and underwater environments;

other types of manipulator a manipulator not belonging to previous definitions.

Fig. 3 shows some examples of the above-defined robot types.

2.2. Query strings details

The Scopus string employed for the first query is the following:
 (TITLE-ABS-KEY ((challenging OR hazardous OR dangerous OR hostile OR harsh OR severe OR contaminated OR confined OR constrained) PRE/2 (environment OR area OR space)) AND TITLE-ABS-KEY (robot OR manipulator OR robotic OR crawler OR drone OR “uav” OR “unmanned aerial vehicle” OR “auv” OR “autonomous underwater vehicle” OR “rov” OR “remotely operated vehicle” OR “ugv” OR “unmanned ground vehicle”) AND TITLE-ABS-KEY (modelling OR model OR control)) AND (TITLE-ABS-KEY (inspection OR maintenance)) AND (LIMIT-TO (LANGUAGE, “English”))

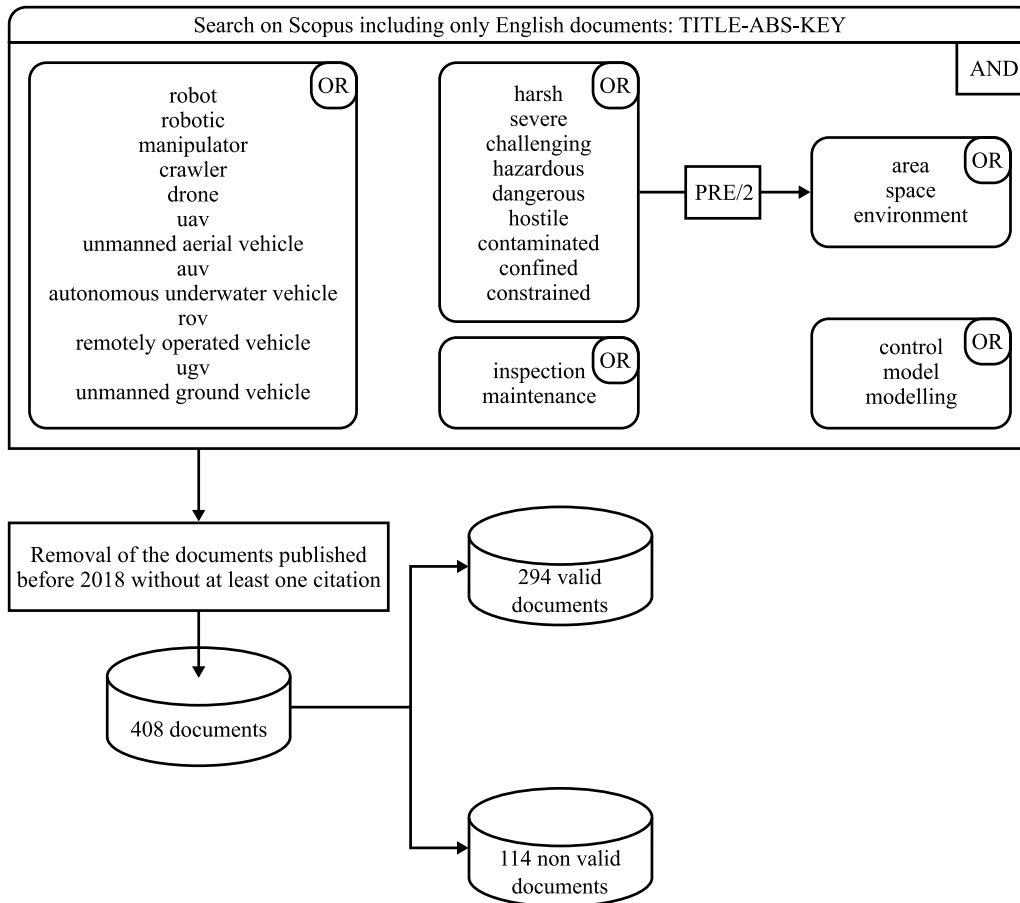


Fig. 1. Schematic of the research procedure for the first query.

The Scopus string employed for the second query is the following: (TITLE-ABS-KEY ((challenging OR hazardous OR dangerous OR hostile OR harsh OR severe OR contaminated OR confined OR constrained) PRE/2 (environment OR area OR space)) AND TITLE-ABS-KEY (“elephant-trunk robot” OR “elephant trunk robot” OR “hyper-redundant robot” OR “hyper redundant robot” OR endoscope OR “continuum robot” OR manipulator OR “robotic arm” OR “robot arm” OR anthropomorphic OR “snake arm” OR “snake-arm” OR “dual arm”)) AND TITLE-ABS-KEY (modelling OR model OR control)) AND (TITLE-ABS-KEY (inspection OR maintenance)) AND (LIMIT-TO (LANGUAGE, “English”))

Since the two queries are designed to find documents focusing on modelling and controlling specific categories of robots for inspection and maintenance in challenging environments, with the same constraints about the language in which the documents are written and the minimum amount of required citation, both the queries share the following:

(TITLE-ABS-KEY ((challenging OR hazardous OR dangerous OR hostile OR harsh OR severe OR contaminated OR confined OR constrained) PRE/2 (environment OR area OR space)) AND TITLE-ABS-KEY (manipulator) AND TITLE-ABS-KEY (modelling OR model OR control)) AND (TITLE-ABS-KEY (inspection OR maintenance)) AND (LIMIT-TO (LANGUAGE, “English”))

Since the two queries focus on different categories of robots, the differences between them reside in the following:

- TITLE-ABS-KEY (robot OR robotic OR crawler OR drone OR “uav” OR “unmanned aerial vehicle” OR “auv” OR “autonomous underwater vehicle” OR “rov” OR “remotely operated vehicle” OR “ugv” OR “unmanned ground vehicle”)
- TITLE-ABS-KEY (“elephant-trunk robot” OR “elephant trunk robot” OR “hyper-redundant robot” OR “hyper redundant robot” OR endoscope OR “continuum robot” OR “robotic arm” OR “robot arm” OR anthropomorphic OR “snake arm” OR “snake-arm” OR “dual arm”)

2.3. Research results

Following the filtering and refining procedure described above, a total of 121 documents remained for the literature review. An analysis was performed to find the discussed topics and the application environments of the manipulators presented by such documents. The following keywords were selected to include the vast majority of possible topics:

control	the document details the robot kinematic and/or dynamic control algorithm;
design	the document provides details about the robot mechanical design;
fault tolerance	the document focuses on the robot’s ability to detect and tolerate internal failures;
modelling	the document provides models and/or simulations concerning the robot;
review	the document presents an overview or directly reviews several robots;
software	the document is about software development or applications;
teleoperation	the document treats teleoperation.

For each document, up to three topics were assigned. Table 1 summarises the topics mentioned in the analysed documents. The following keywords were selected to include all possible application environments:

aviation	the main application is in the aviation sector;
-----------------	---

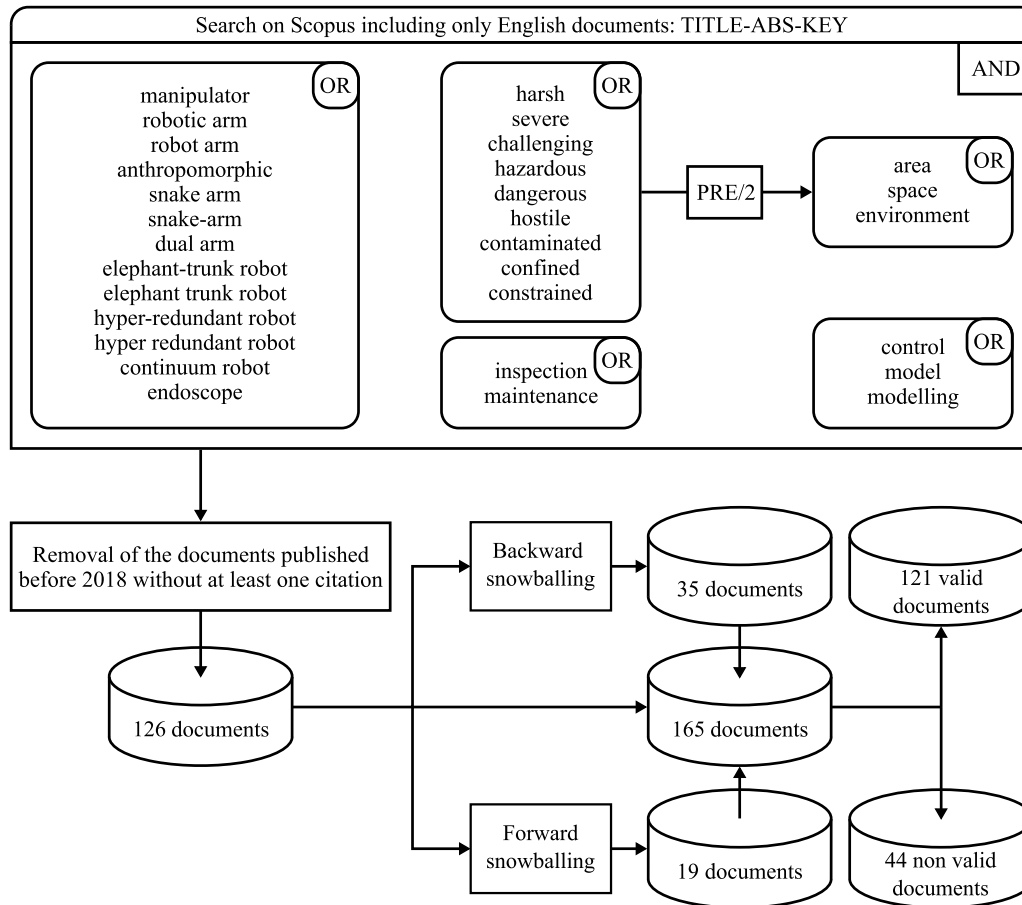


Fig. 2. Schematic of the research procedure for the second query.

- confined and constrained** the robot operates in generic confined and constrained environments;
- energy** the main application is in the energy (production and distribution) sector;
- general-purpose** the robot performs general-purpose inspection or maintenance activities;
- industry** the main application is in the industry sector;
- medicine** the main application is in medicine;
- not specific** no specific sectors are mentioned in the document;
- nuclear** the main application is in the nuclear sector;
- oil and gas** the main application is in the oil and gas sector;
- space** the robot operates in space.

For each document, only one application environment was assigned. Table 2 summarises the application environments of the manipulators proposed in the analysed documents.

3. Discrete-Joint Hyper-Redundant Manipulators

In this work, a DJHRM is defined as a fully-actuated or over-actuated manipulator, i.e. each of the DoF of the robot is driven by at least one motor, where the number of DoF of the manipulator is higher than the DoF required by a given task. The literature review reveals that

Table 1

Summary of the documents topics. For each robot type, the column [#] reports the absolute number of documents per topic, the column [%] reports the percentage of documents per topic. Since up to three keywords are assigned to each document, columns [%] are not normalised.

Topic	Discrete-joint		Continuum		Mobile		Other	
	[#]	[%]	[#]	[%]	[#]	[%]	[#]	[%]
control	29	69	24	73	13	52	16	75
design	16	38	20	61	8	32	5	24
fault tolerance	5	12	0	0	0	0	0	0
modelling	20	48	26	79	5	20	9	43
review	0	0	0	0	4	16	0	0
software	0	0	0	0	3	12	2	10
teleoperation	1	2	3	9	12	48	7	33

DJHRMs are a leading technology when manipulation or inspection is required in confined and hostile environments. As confirmation, nuclear-related industry is the major sector supporting the research on DJHRMs.

The high number of DoF allows DJHRMs to follow a desired trajectory in confined spaces while simultaneously achieving other tasks, e.g. avoiding obstacles, satisfying joint angles limit, or avoiding singularities. Furthermore, the kinematic redundancy makes DJHRMs intrinsically fault-tolerant and particularly suitable for operating in hazardous environments. Although kinematic redundancy makes these robots attractive for inspection and maintenance tasks, it must be appropriately managed to achieve the desired performance.

The nuclear-related industry often requires maintenance and inspection in large and constrained environments. Since long structures are subject to high deformation and propagation of errors due to



Fig. 3. Examples of the robot classification: (a) The robot proposed by Canali et al. (2022). (b) The robots proposed by Almagro et al. (2020). (c) From ©2017 Elsevier. Reprinted, with permission, from Dong et al. (2017).

Table 2

Summary of the manipulators application environments. For each robot type, the column [#] reports the absolute number of documents per application environment, the column [%] reports the percentage of documents per application environment. Since only one keyword is assigned to each document, columns [%] are normalised to 100 %.

Application environment	Discrete-joint		Continuum		Mobile		Other	
	[#]	[%]	[#]	[%]	[#]	[%]	[#]	[%]
aviation	1	2	9	28	0	0	0	0
confined and constrained	11	26	3	9	1	4	0	0
construction	0	0	0	0	0	0	1	5
energy	1	2	0	0	1	4	4	19
general-purpose	8	19	4	12	12	48	1	5
industrial	0	0	0	0	2	8	3	14
medicine	0	0	7	21	0	0	1	5
not specific	5	12	10	30	3	12	1	5
nuclear	9	22	0	0	4	16	6	28
oil and gas	0	0	0	0	1	4	0	0
space	7	17	0	0	1	4	4	19

uncertain parameters, several compensation methods have been studied to guarantee the desired performance.

This section gives an insight into the key issues addressed over the years to develop DJHRMs for harsh environments inspection and maintenance. Section 3.1 describes the different designs developed for several sectors. Section 3.2 presents the modelling techniques used to describe the kinematic and dynamic behaviour of DJHRMs. Section 3.3

illustrates different kinematic and dynamic control schemes developed to deal with kinematic redundancy and improve the performance of DJHRMs.

3.1. Design

Over the years, several designs of DJHRMs have been proposed to perform specific tasks, e.g. the need to carry tools or inspection

equipment in a large but constrained environment, such as a nuclear reactor or a Tokamak, led researchers to explore designs that reduce the mass of the manipulator and compensate for the torque induced by gravity. These specifications are typical in DJHRMs. A widespread design choice for addressing these requirements is cable actuation, which moves the actuators from the joints to the chassis, reducing the mass of the moving structure. In addition, locating the actuators further from the hazardous environment reduces the risk of faults since electronic boards are sensitive to high temperatures and radiation. Recent studies on synthetic fibre cables, by [Horigome and Endo \(2018\)](#), show that, for the same tensile strength, these cables have a much lower mass and higher durability against sharp bending than stainless steel cables.

One of the first examples of a DJHRM is the CT Arm developed by [Ma, Hirose, and Yoshinada \(1994\)](#). The CT Arm, designed for the maintenance of nuclear reactors, is a 9-DoF planar manipulator that uses coupled tendon mechanisms to distribute the power supplied by each electric motor on all the joints avoiding concentrating the load on a single actuator. Consequently, actuators of reduced size and power can be employed. Using the CT Arm as a baseline, [Horigome et al. \(2014\)](#) enhanced the coupled tendon mechanism to obtain a manipulator able to move in 3D space. [Endo, Horigome, and Takata \(2019\)](#) used the mechanism designed by [Horigome et al. \(2014\)](#) to develop Super Dragon, a 10-m-long manipulator for decommissioning the Fukushima Daiichi nuclear power plant. Super Dragon has 10 revolute joints actuated by 20 cables connected to the same number of DC motors. In addition to the coupled tendon mechanism, Super Dragon has an additional tendon to compensate for the gravity. This tendon, driven by a pneumatic linear actuator, acts on the first five joints of the manipulator, which allows motion only on the plane where the gravity vector lies. A double pulleys mechanism is employed to apply the appropriate weight compensation on each joint. Coupled tendon mechanisms considerably reduce the size and power of actuators by distributing the loads applied on each joint to all the actuators but require many pulleys on each joint, leading to an increase in the size of the arm diameter.

One of the most common cable-driven designs is based on connecting several modules in series through universal joints, each actuated by three cables. This design provides two DoF to each module, increasing the manipulator's ability to follow complex trajectories. In addition, it removes pulleys from the joint axes and simplifies the cable routing along the arm. However, it does not provide any gravity compensation mechanism reducing the maximum arm length. The literature provides several studies based on this design that differ in the number of modules and arm lengths. [Xu, Liu, and Li \(2018\)](#), [Tang et al. \(2019\)](#), [Zheng et al. \(2021\)](#), and [Qin, Wang, et al. \(2023\)](#) presented some examples of DJHRMs with universal joints actuated by three cables.

The cable-driven DJHRM designs described previously are over-actuated. Over-actuated mechanisms require implementing complex algorithms to find the force to apply on each cable to avoid slack cables or to generate high reaction forces. Furthermore, the high number of actuators required increases the production costs and the probability of faults. Several designs have been proposed to obtain fully-actuated cable-driven DJHRMs. [Marais and Göktogan \(2017a\)](#) presented the Cable-driven Remote Access Manipulator (CRAM) developed for inspecting and maintaining the internal structure of aircraft wing-frames. The design is based on connecting several identical modules through universal joints. A single actuator drives each DoF of the robot by exploiting pulleys and the cable routing along the arm through Bowden tubes. A pretensioning mechanism must be included in the base of CRAM to prevent cable slacks during the manipulator motion. [Canali et al. \(2022\)](#) presented the Snake-Like manipulator for Inspection and Maintenance (SLIM). SLIM is a planar cable-driven DJHRM composed of 12 modules, a pan and tilt mechanism acting as end-effector, and a rotating actuation box, around which the arm can wrap. This 15DoF robot, is designed for harsh environments, and can deploy up to about

4.8 m. Each module comprises a rigid link and a pulley acting as a revolute joint. Each pulley is driven by a cable constrained to pass along the neutral axis of each link through rollers. This routing strategy allows driving each joint through a single linear actuator. [Guardiani et al. \(2022\)](#) presented a novel gear transmission joint mechanism designed to develop a fully-actuated cable-driven DJHRM without employing any pulley to transfer the motion from the actuators. The gear transmission joints constrain two antagonist cables, which drive each module of the manipulator, to satisfy a kinematic law that employs a single linear actuator for each DoF. [Huang, Yan, Yang, Hu, and Xu \(2023\)](#) and [Taiwei, Huang, Wenfu, Ke, and Liang \(2023\)](#) proposed a fully-actuated cable-driven DJHRM based on quaternion joints. Quaternion joints are parallel mechanisms designed by [Kim, Kim, and Jang \(2018\)](#) that allow approximating a 2-DoFs spherical rolling motion. Therefore, the motion of the antagonist cables in this joint is symmetric avoiding slack cables and their excessive stretching, allowing to employ a single actuator per DoF.

Although most DJHRMs have cable actuation, there are some designs with actuators mounted on the arm. The Jet Propulsion Laboratory (JPL) Serpentine Robot, by [Paljug, Ohm, and Hayati \(1995\)](#), is a 12-DoF manipulator designed for space application. Each joint has two DoF and comprises an internal universal joint and an external gear-bearing-gear mechanism. [Villedieu et al. \(2016\)](#) developed a long-reach DJHRM, the Articulated Inspection Arm (AIA). Its design, described by [Chalfoun, Bidard, Keller, Perrot, and Piolain \(2007\)](#) and [Keller et al. \(2008\)](#), allows for movement in the extreme conditions of a vacuum vessel of a fusion Tokamak, i.e. high temperature, high radiation, and ultra vacuum pressures. AIA is a 9.5 m long manipulator comprising five identical modules with a diameter of 0.16 m. Each module comprises two revolute joints: the pitch angle, obtained through a four-bar mechanism, and the yaw angle, driven by a cable and pulleys mechanism. An additional DoF is provided by a linear actuator that allows the insertion into the vacuum vessel. The four-bar mechanism maintains the yaw rotation axis parallel to the gravity vector, and a spring mechanism mainly compensates for the gravity force acting on the pitch axis. These mechanisms significantly reduce the power the actuators must provide to counteract the gravity force.

The high number of DoF of DJHRMs can be exploited during the design phase to develop fault-tolerant manipulators. Fault-tolerant manipulators are crucial in extreme and hazardous conditions. This design paradigm exploits the relationship between dexterity and the Jacobian matrix to define a robot geometry that guarantees dexterity and mobility even if some actuators fail. [Ben-Gharbia, Maciejewski, and Roberts \(2013\)](#) proposed a method to find a family of locked-joint failure tolerant 4-DoF manipulators, which are redundant for positioning the end-effector. This property is obtained by ensuring that the manipulator's Jacobian matrix has equal singular values.

3.2. Modelling

The literature review reveals that the two main aspects studied in DJHRMs are the relations between the actuators and the end-effector motion, i.e. kinematic models, and the actuation forces necessary to counteract the forces applied on the robot, i.e. static and dynamic models.

3.2.1. Kinematic modelling

The most common kinematic model for cable-driven DJHRMs consists of a multilevel map. In general, the multilevel map is employed when the joints of a robot are not directly driven by a motor and a specific map is needed to describe the relationship between actuators and joints motion. Therefore, it is usually composed of two maps, the one between the actuation space and the configuration space, which depends on the mechanical design of the manipulator, and the one between the configuration space and the task space, which is independent from the mechanical design, but only on the kinematic chain of

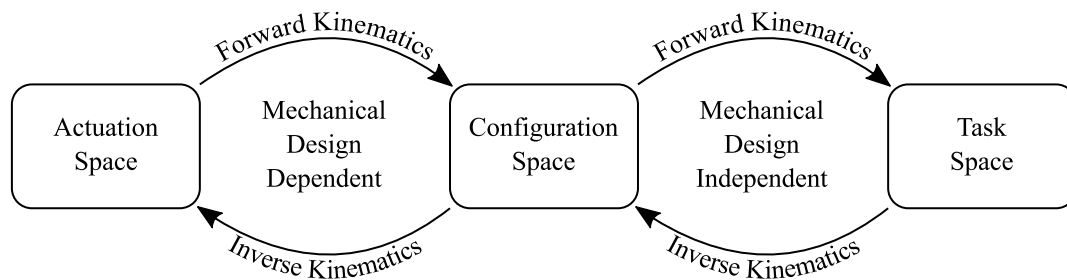


Fig. 4. Schematic of a general multilevel kinematic map.

the manipulator. Fig. 4 represents the scheme of a general multilevel map. In particular, for cable-driven manipulators, the map between the actuation space and the configuration space corresponds to the cable length space to joint space kinematic map, while the map between the configuration space and the task space corresponds to the joint space to end-effector space kinematic map. The joint space to end-effector space kinematic map is computed through a combination of homogeneous transformation matrices according to the geometry of the manipulator. The cable length space to joint space kinematic map is obtained through geometric relations between the points on the flanges in which the cables are constrained to pass during the motion of the joints. While the joint space to end-effector space kinematic map can be solved using the same algorithm on different designs, the cable length space to joint space kinematic map strictly depends on the joints mechanical design. Consequently, for each design, it is necessary to define the corresponding map. Xu et al. (2018), Tang et al. (2019), Zheng et al. (2021), and Qin, Wang, et al. (2023) described the kinematic model of cable-driven DJHRMs with each module connected through universal joints and driven by three cables. Huang et al. (2023) and Taiwei et al. (2023) described the kinematic model of a cable-driven DJHRM composed of quaternion joints. The proposed kinematic model is defined under the assumption that the quaternion joint behaves like an ideal spherical rolling joint. This assumption introduces an approximation error in the kinematic model. Guardiani et al. (2022) presented the kinematic model for a cable-driven DJHRM with gear transmission. Horigome et al. (2014) illustrated the kinematic model for a cable-driven DJHRM that exploits the coupled tendon principle. A common aspect of the kinematic map of these designs is that motion of the joints is coupled, i.e. the motion of a single joint induces a motion on the subsequent joints.

DJHRMs with onboard actuators have kinematics that strictly depends on their designs. Paljug et al. (1995) defined two equivalent kinematic models using homogeneous transformations. One is obtained by defining the frames on the universal joints, while the other defines the frames on the gear-bearing-gear mechanisms. Chalfoun et al. (2007) presented a kinematic model based on homogeneous transformation, which also considers the deformation of each module due to the gravity force.

Due to the high number of modules and the length of DJHRMs, the propagation of the geometric parameters uncertainties significantly reduces the end-effector positioning accuracy. Parameters identification procedures, to calibrate the manipulators' kinematic model, can significantly improve their positioning accuracy. Zheng et al. (2022) presented a least-square algorithm to calibrate the Denavit–Hartenberg (DH) parameters of a DJHRM with modules connected through universal joints and driven by three cables each. This method can calibrate the tip of each module to improve not only the end-effector trajectory tracking but also the positioning of each module tip.

Fault tolerance is an interesting feature of DJHRMs and several studies have proposed models to describe and measure this feature. Lewis and Maciejewski (1997), Ben-Gharbia et al. (2013), and She, Xu, Su, Liang, and Shi (2016) exploited the singular values of the Jacobian matrix of a manipulator to define indicators that quantify robot's fault

tolerance. English and Maciejewski (1998) proposed several failure-susceptibility measures based on torque, acceleration, and angle position that can detect failure conditions.

3.2.2. Static and dynamic modelling

Most studies that describe the actuation forces of DJHRMs assume that the robot's velocity is small enough to make the inertial forces negligible, consequently presenting static models. Chalfoun et al. (2007) illustrated how the gravity force distributes on the four-bar linkage mechanism and the gravity compensation spring of the AIA robot. Furthermore, this work presented a lumped parameters model describing the manipulator structure's deformation under gravity. Endo et al. (2019) presented a model that computes the cable forces of a coupled tendon DJHRM. The cable forces and the weight compensation tendon balance the gravity torque. However, since the system is over-actuated, the authors proposed an optimisation procedure to minimise cable forces, avoiding slack cable and failure. Guardiani et al. (2022) proposed a model that also includes the cable routing in the static model of the robot. The cable forces are computed iteratively using the Newton-Euler method. This model forms the baseline for a cable routing optimisation algorithm that minimises the actuator forces and range of motion. Qin, Wang, et al. (2023) computed the cable forces by solving the force and torque balance equation considering only gravity.

Xu et al. (2018) presented a dynamic model for cable-driven DJHRMs with modules connected through universal joints and driven by three cables. The actuation forces are computed iteratively through the Newton-Euler method. This model includes cable tension, cable contact forces, cable friction, link gravitational forces, link inertia forces, and adjacent link interaction forces. Since this manipulator is over-actuated, an optimisation algorithm is employed to minimise the cable forces required to perform a desired movement. For the same type of cable-driven DJHRMs, You, Liu, and Ma (2023) proposed a multi-body dynamic model that includes clearance and friction of cables. The arbitrary Lagrangian Euler method, a simplified one-dimensional finite element modelling technique, is used to derive the cable dynamics. This model can describe the cable slack phenomena due the coupling effects of clearance and friction. De Mari Casareto Dal Verme, Ludovico, Pistone, Canali, and Caldwell (2023) proposed a dynamic model for cable-driven DJHRM which includes the visco-elastic behaviour of synthetic fibre cables. This model accurately describes the dynamics of synthetic fibre cables that can be used in designing model-based dynamic controllers. Meng, Xu, Xu, Sun, and Liang (2023) used the principle of virtual work to establish the dynamics of a long-reach cable-driven DJHRM for space application. The manipulator considered in this work transmits the motion from the actuators to the joints through a capstan drive. Therefore, the proposed model included the capstan drive equation and the elastic behaviour of cables.

3.3. Control

The literature review shows that the main topic investigated in controlling DJHRMs is the kinematic redundancy and, consequently, the kinematic control. This exploits the full potential of hyper-redundancy

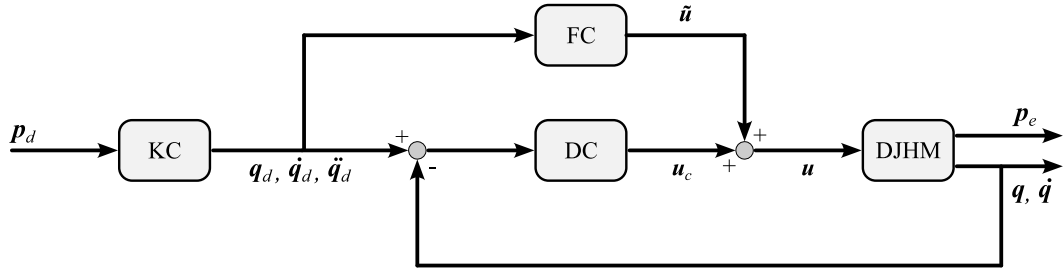


Fig. 5. Generic control scheme for DJHRM that includes the kinematic controller, KC, the feed-forward controller, FC, and the dynamic controller, DC. The signals p_d and p_e are the desired and actual end-effector position, respectively. The kinematic controller computes the desired joint angular position q_d , velocity \dot{q}_d , and acceleration \ddot{q}_d . The actual joint angular position and velocity are defined as q and \dot{q} , respectively. The control signal u is computed as the sum of feed-forward command \tilde{u} and the feedback command u_c .

to perform tasks in confined and constrained environments. However, if high trajectory tracking performance is required, kinematic control alone is not sufficient and dynamic controllers, which often includes also feed-forward controllers, may also be needed. Fig. 5 shows a block diagram describing a general control scheme which includes kinematic, dynamic, and feed-forward controllers.

3.3.1. Kinematic control

If adequately handled, kinematic redundancy allows manipulators to avoid singularities, environmental obstacles, and joint limits. Several kinematic control algorithms have been proposed to deal with kinematic redundancy.

Jacobian-based algorithms, studied since the 1980s by Sciavicco and Siciliano (1988), exploit the null space of the Jacobian matrix to include secondary tasks. Marais and Göktogan (2017b) implemented a damped least-squares technique to solve the inverse kinematic of DJHRMs presenting a novel manipulability index to detect when a singularity occurs. This index acts as the variable damping coefficient in the damped least-squares algorithm and give a smoother damping behaviour. Bláha and Svejda (2018) proposed a Jacobian-based algorithm to perform motion on cylindrical surfaces like pipes. Performing a change of coordinates to project the six DoF end-effector coordinates to the pipe surface, it is possible to solve the inverse kinematic problem using Jacobian-based methods in the developed view of the surface of the pipes, which requires only four coordinates to be represented instead of the six of the Cartesian space. Canali et al. (2022) implemented a Jacobian-based algorithm in which the trajectory tracking task has the lowest priority ensuring that the DJHRM first satisfies the joints limits and then avoids any collision. Most of the Jacobian-based algorithms proposed in the above-mentioned works exploit the properties of the null space of the Jacobian matrix to achieve multiple tasks with different priority. This method is based on making explicit the self motion of the manipulator in the inverse differential kinematics as:

$$\dot{q} = J_1^\dagger v_1 + \sum_{i=2}^{N_t} \left[\prod_{k=1}^{i-1} (I - J_k^\dagger J_k) \right] J_i^\dagger v_i, \quad (1)$$

where N_t is the number of tasks to accomplish simultaneously, \dot{q} is the joint velocity, v_i is the desired velocity of the i th task, J_i is the Jacobian matrix associated with the i th task, \dagger indicates the Moore–Penrose inverse of a generic matrix, and the operator $(I - J_k^\dagger J_k)$ is the kernel of the Jacobian matrix associated to the k th task. Thus, by implementing Eq. (1) in discrete time, it is possible to compute the desired joint configuration at the time instant t as

$$q_t \simeq q_{t-1} + J_1^\dagger e_1 + \sum_{i=2}^{N_t} \left[\prod_{k=1}^{i-1} (I - J_k^\dagger J_k) \right] J_i^\dagger e_i, \quad (2)$$

where q_{t-1} is the joint position at the previous time instant and e_i is the position error of the i th task.

Jacobian-based methods become computationally expensive when the number of DoF increases. Therefore, geometric methods to solve

inverse kinematic problems have been proposed to reduce the computational costs. Huang et al. (2023) proposed a geometric method to solve the inverse kinematics of a cable-driven DJHRM composed of quaternion joints. Exploiting the ideal spherical rolling motion of quaternion joints, a simplified kinematic model is obtained as a series of isosceles trapezoids that share a common non-parallel side. From this model, a geometric iteration approach based on the Forward And Backward Reaching Inverse Kinematics (FABRIK) method, developed by Aristidou and Lasenby (2011), is performed to solve the inverse kinematic problem. The FABRIK method, instead of using rotation matrix and Jacobian, solves the inverse kinematic problem by finding the joint locations on the line which passes through the target position and the end-effector of the manipulator. Fig. 6 shows a complete iteration of the FABRIK algorithm. Niu, Han, Huang, and Yan (2024) proposed an improved FABRIK method to solve both the position and orientation inverse kinematic problems in a single-layer iteration. The proposed algorithm deals with joint limits and navigation into narrow environments. Ju et al. (2022) proposed to solve the inverse kinematic problem of a cable-driven DJHRM composed of universal joints actuated by three cables by improving the FABRIK method to consider joint constraints and a segmented control strategy to exploit the redundancy of DJHRM in constrained environments. The proposed algorithm exploits the solution of each iteration of the FABRIK method to generate the intermediate end-effector points in a point-to-point motion. During an iteration, the maximum joint angle increment is limited by velocity and geometric constraints. The obstacle avoidance is then obtained using a segmented inverse kinematic strategy. The manipulator is divided in three parts, the anterior from joint 1 to joint n , the middle from joint n to joint m , and the posterior from joint m to the end-effector. The position of joint n is changed to avoid the obstacle, then by applying the FABRIK method on the three sub-manipulators the inverse kinematics of the entire robot is obtained. Martín-Barrio, Roldán-Gómez, Rodríguez, Del Cerro, and Barrientos (2020) solved the inverse kinematic problem using a geometric method called the natural Cyclic Coordinate Descent (CCD) method, described by Martin, Barrientos, and Del Cerro (2018). This iterative method moves one joint at a time to minimise the end-effector position error. Fig. 7 shows two iterations of the CCD algorithm. In addition, the robot is driven in a virtual environment using mixed-reality (MR) tools. With the help of a head-mounted display, the operator can move the robot by dragging each joint to reach the desired pose. Having defined the target pose, the operator transfers the resulting trajectory to the real robot that executes the task remotely. Qin, Wu, and Ji (2023) proposed a follow-the-leader algorithm to compute the inverse kinematic of a DJHRM. This approach is based on knowledge that, as the manipulator moves forward, all the sections follow the manipulator tip path, as explained by Xie, Wang, Li, Hu, and Yang (2019). A similar approach is the path follow method where all the joints of a DJHRM are kept on a desired path with minimal error. Wang, Xie, and Yang (2023) proposed a new heuristic path follow method that finds the joint position through a geometrical approach, and then moves iteratively the joints to satisfy

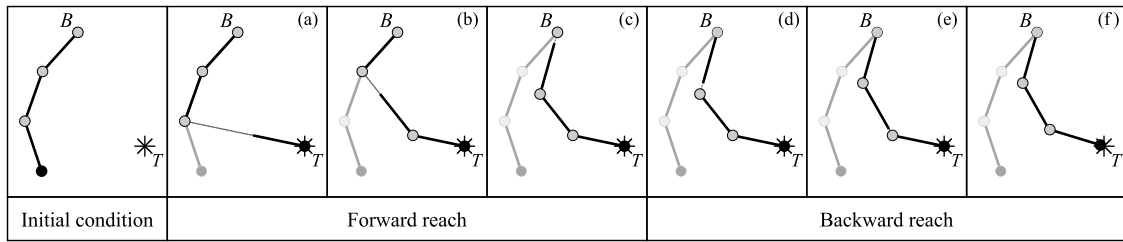


Fig. 6. Geometric representation of a single complete iteration of the FABRIK algorithm on a 3-joints planar manipulator. Points B and T represent the base of the manipulator and the target position of the end-effector, respectively. The grey and black circles represent the joints of the manipulator and its end-effector, respectively.

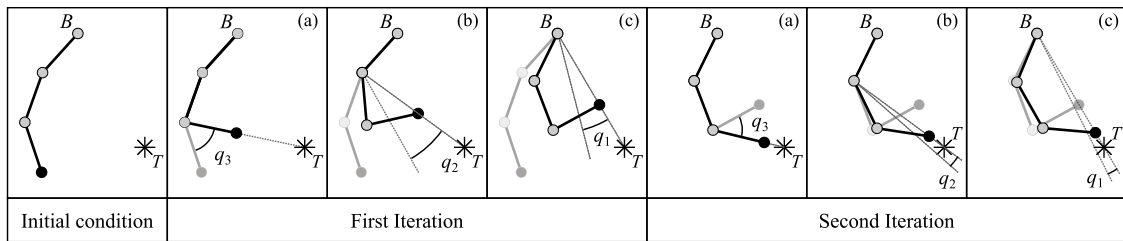


Fig. 7. Geometric representation of two complete iterations of the CCD algorithm on a 3-joints planar manipulator. Points B and T represent the base of the manipulator and the target position of the end-effector, respectively. The grey and black circles represent the joints of the manipulator and its end-effector, respectively. The angle q_i is the rotation angle applied at the joint i th during each iteration of the algorithm.

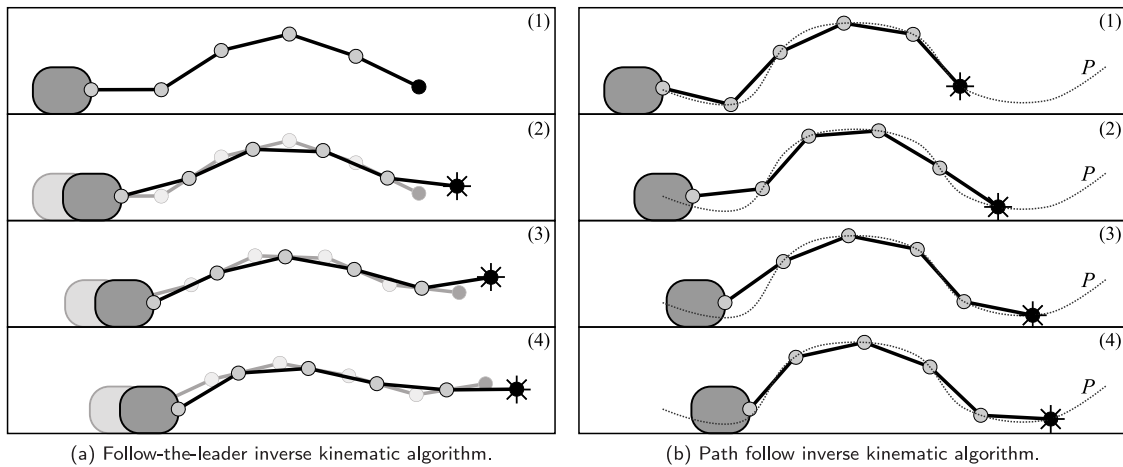


Fig. 8. Four frames of a DJHRM performing the follow-the-leader (a) and path follow (b) inverse kinematic algorithms. The follow-the-leader algorithm moves the end-effector to the desired target point, identified by a star, trying to move simultaneously all the joints on the link of the manipulator in the previous configuration. The path follow algorithm tries to move all the joints on the curve defined by the desired path P .

their limits. Fig. 8 shows a comparison between the trajectory obtained with the follow-the-leader and the path follow algorithms.

Tang et al. (2019) proposed a geometric method to solve the inverse kinematics in real-time. Mu et al. (2019) proposed a novel geometric inverse kinematic method for DJHRMs that introduces follow-up controlled points, one every four DoF of the robot, and the same number of active control points. This method allows for obstacle avoidance and end-effector trajectory tracking by minimising the distance between the nodes and the control points. Peng, Zhang, Meng, and Liang (2023) proposed a vision based inverse kinematics approach. The authors suggested a trajectory optimisation method, which, starting from sensing the arm shape through a multi-camera fusion algorithm, exploits a particle swarm optimisation algorithm to find the optimal shape to follow a desired trajectory considering configuration, manipulability, and joint angle constraints.

Long mechanical structures, like DJHRMs for maintenance and inspection, are subject to high deformations due to their flexibility and the high load induced by gravity. Several studies have used machine learning techniques to improve the performance of kinematic control

algorithms. Shi, Cheng, Pan, Zhao, and Wu (2018) proposed a method to calibrate and compensate in real-time for the error due to the uncertain geometric parameters of the AIA. The deflection and rotation of the tip of a single module are measured through a laser scanner when a specific pitch angle and an external load are applied. The measured data are used to train a Back Propagation Neural Network (BPNN) that, given the pitch angle and the load applied on the module's tip, can predict the deformation of each module to compensate for the deformation in real-time. Ludovico et al. (2021) illustrated two methods based on neural networks to compensate for cable deformation comparing the results with a model-based approach. These authors proposed to implement an Artificial Neural Network (ANN) to map the joint space coordinates into actuator space coordinates, i.e. the ANN allows computing the linear displacement of the actuators to obtain the desired joint angles. The ANN takes the measured joint angles as input and returns the linear displacement of the actuators as output. Better performance can be obtained by implementing a Recursive Artificial Neural Network (RANN) since it updates the network weights during

the execution of a task. Yao et al. (2022) studied a method to compensate for the deformation of the Multipurpose Overload Robot (CMOR), the principal part of the remote handling system of the China Fusion Engineering Test Reactor (CFETR). The CMOR is a 9-DoF DJHRM with actuators, which can carry a payload of up to 2000 kg, arranged along its 10.8 m length arm. Deformations of up to 140.8 mm are possible during the operation in the CFETR. The deformation model is based on a BPNN trained through a Finite Element Analysis (FEA). The BPNN takes as inputs the joint angles and the load applied and returns as outputs the displacement of the end-effector due to the deformation. This deformation model is used in the control loop for real-time compensation.

Interesting results are obtained by exploiting hyper-redundancy to define kinematic control methods that are fault tolerant. Lewis and Maciejewski (1997) presented a method which defines artificial joint limits computed from the intersection of self-motion manifolds of DJHRMs with a locked joint failure. These artificial joint limits help achieving critical tasks even if a locked joint failure occurs. Jamisola, Maciejewski, and Roberts (2006) extended this method to consider the presence of obstacles and generate collision-free fault-tolerant trajectories. English and Maciejewski (1998) proposed a mathematical framework for establishing failure-susceptibility measures that can be employed as secondary cost functions to optimise under the constraint of completing a primary task. The proposed method defines torque-based, acceleration-based, and swing-angle-based susceptibility measures that can be exploited in the extended-Jacobian method to find a fault-tolerant inverse kinematic solution.

3.3.2. Dynamic control

Dynamic controllers can considerably increase position accuracy. Xu et al. (2018) proposed a dynamic controller based on the kinematic and dynamic equations describing a cable-driven DJHRM with modules connected through universal joints, each driven by three cables. First, given a desired trajectory, the corresponding motor angles are computed through the kinematic model. Then, each motor is controlled through the PD control algorithm plus feed-forward compensation. The feed-forward model is computed using the Newton-Euler method. Endo et al. (2019) implemented a dynamic controller that considers only the static force model. The control algorithm consists of two PI controllers that regulate the joint angles and the cable forces. The desired cable forces are computed through an optimisation algorithm which minimises the force avoiding slack cables. Zheng et al. (2021) described a puller-follower control algorithm that simultaneously controls the position of the puller cables and the force of the follower cables. Huang et al. (2023) proposed a PID plus feed-forward controller for a cable driven DJHRM composed of quaternion joints. The desired motion of the cables is used as feed-forward term and the PID controller is implemented to close the joint position loop. A threshold on the integral action is employed to avoid oscillation effects due to the delay of the cable transmission. Canali et al. (2022) proposed a dynamic controller inspired by the hysteresis phenomenon to reduce the vibration in a cable-driven DJHRM. The proposed algorithm takes as input the angular error and returns the desired motor velocity. The sinusoidal disturbance rejection is obtained by applying as reference piece-wise constant velocity. This algorithm gives precise position control while minimising the cable forces. De Mari Casareto Dal Verme et al. (2023) proved the stability in sense of Lyapunov of a cable-driven DJHRM with a non-linear full-state feedback controller that considers the visco-elastic behaviour of synthetic fibre cables. The proposed controller can be applied on cable-driven DJHRMs under the assumption that the actuation system is composed of two synthetic fibre cables per joint, routed along the robotic arm so that the map between the linear velocity of the cables and the angular velocity of the joints is constant and decoupled. Luo, Hu, Zhang, and Sun (2022) proposed an inverse dynamics segmented hybrid motion-force control for space

applications. The DJHRM is divided in two segments. A hybrid motion-force controller is used in the first segment to exploit the interaction with the environment to make the manipulator more stable. A pure motion controller is applied on the second segment to accomplish positioning tasks. Meng et al. (2023) designed a trajectory tracking control scheme based on a time-delay estimation and non-singular terminal sliding mode control for a long-reach cable-driven DJHRM for space application. The time-delay approach is used to estimate the dynamic inertia of the manipulator, while the terminal non-singular allows to stabilise the system and guarantee desired performance. Peng, Zhang, Ge, and Han (2022) proposed two vision feedback based trajectory tracking controls for a cable-driven DJHRM composed of universal joints actuated by three cables for space application. The first controller is basically a PD plus inverse dynamic controller with vision feedback in which the model uncertainties of the multilevel mapping between actuators, cables, joints, and the operational due to cables deformation is considered. The second controller implements an iterative learning control to exploit the manipulator redundancy and optimise the trajectory tracking.

Dynamic control algorithms can also manage joint failures. She et al. (2016) exploited the condition number, the manipulability index, and the minimum singular value to define a safe region where the manipulator could perform a desired task. When a failure occurs, the damaged joint is free to move, and the manipulator becomes underactuated. Despite this, it is possible to move and subsequently lock the malfunctioning joint into the desired safe region while continuing to perform the desired task by exploiting the underactuated dynamics and the self-motion ability of DJHRMs. Modelling accuracy is crucial when controlling an underactuated system and an H_∞ control algorithm addresses all the possible modelling uncertainties.

4. Continuum manipulators

Unlike DJHRMs, continuum manipulators have a vast number of DoF that are not singularly actuated. The number of DoF is considered tending to infinite or even infinite in the case of compliant joints made of flexible materials. The large number of DoF and the possible mechanical compliance make continuum robots able to move and operate inside confined spaces, which is a crucial feature for many practical applications, like minimally invasive surgery, aero-engine maintenance, and aircraft assembly. The literature review reveals that continuum manipulators are good solutions especially for the aviation industry, for maintenance of engines and fuel tanks, and medicine, for endoscopy or surgery. More than half of the retrieved studies, in fact, are focused on these applications, while the remainder consider continuum manipulators designed for generic constrained environments.

Continuum manipulators usually consist of several small bendable segments composed of a joint or a backbone that connect all the robot segments, which are actuated in groups. Many actuation strategies are possible, including hydraulic or pneumatic actuation. However, the research described in Section 2 shows that the most common strategy is cable actuation, which has the advantage of generating an output force capable of highly increasing robot payload capability. An important example of cable-driven continuum manipulator for inspection in challenging environments is the snake-arm robot from OC Robotics, described by Buckingham and Graham (2012).

The combination of joints, backbones, and actuation determines the manipulator's motion capability and mechanical compliance. The robot design is generally driven by the specific application. Besides the distinction between robots able to move within a 3D space or those constrained to move in one plane, continuum manipulators are also characterised by their specific motion shape capabilities, like the C-c bending shape or S-bend shape implemented by Wang et al. (2021) and Dong et al. (2017), respectively.

Given the vast number of DoF, kinematic modelling of continuum manipulators is complex and forms one of the main research directions

when dealing with these robots. As in the case of DJHRM, for continuum manipulators actuated from their base, the kinematic modelling must include the two maps schematised in Fig. 4: (i) the map between the task space and the configuration space, which is independent from the robot design, and (ii) the map between the configuration space and the actuation space, which strongly depends on the mechanical design of the robot and on the actuation approach, e.g. cable actuation, pneumatic actuation, or water actuation. However, the literature review revealed also a few researches in which dynamic models of continuum manipulators were defined and exploited to define control strategies.

To control continuum manipulators, the literature identifies several strategies, which can be divided into two families: open-loop and closed-loop control. The former is usually applied when the robot size prevents sensors integration into the manipulator and mainly relies on inverse kinematics and static models of the manipulator. The latter includes both model-based and model-free control strategies.

This section studies the main topics about continuum manipulators. Section 4.1 considers their mechanical design, Section 4.2 presents an overview of the strategies to model continuum manipulators, and Section 4.3 describes the control techniques applied.

4.1. Design

Continuum manipulators usually consist of some bending sections, each one composed of several bending segments. These segments are often composed of a rigid disk (sometimes called ring, vertebra, or spacer) and a joint that allows the bending behaviour of the structure.

Another key element of continuum robots is the backbone, i.e. the element that connects all the segments of all the sections of the robot. In many cases, especially when a compliant joint is employed, the joint acts as a backbone itself, but sometimes a separate backbone is necessary or useful to obtain a particular performance. Unlike DJHRMs, continuum manipulators joints are not individually actuated: the actuation, indeed, is at the section level, which means that the joints are actuated in groups. Exploiting these concepts, key design differences are primarily in the actuation strategy and in the materials and structures of the joints and backbones.

As already mentioned, most continuum manipulators are cable-driven. In fact, in this study only three robots are actuated differently: the first is a manipulator for intra-cavity tasks actuated via a dual continuum mechanism and presented by Xu, Mei, Yang, Han, and Zhu (2014). This design consists of four sections, each composed of a base ring, several spacers, an end ring, and a set of super-elastic rods. The rods act as backbones and each group of backbones is attached to the end ring of a section. The robot is actuated by pulling and pushing directly the backbones driving the corresponding section. A later version of this robot was used in the aviation industry by Liu, Yang, et al. (2016). The second non-cable driven design is a pneumatic-actuated robot, designed by Talas, Baydere, Altinsoy, Tutcu, and Samur (2020). It is a growing soft robot able to move via elastic elongation and by adding material to its tip by conveying to it the deflated tubings. This robot can bend in three axes and a translate along one. The third design is a waterjet-actuated continuum endoscope, called HydroJet Endoscopic Device and presented by Campisano, Ramirez, Landewee, et al. (2020). This system is designed for the inspection of the upper gastrointestinal tract and is divided into two main parts: the active soft elastomer sleeve and the passive multilumen catheter. The sleeve is actuated by three flexible tubes carrying pressurised water from the catheter to the jets. The forces produced by the waterjet actuation system allow the soft sleeve to bend within a relatively small workspace.

For the cable-driven robots, since mechanical compliance is essential to operate in constrained environments, most designs have flexible joints. Indeed, just two of the robots in the literature review have rigid joints. The first, developed by Yeshmukhametov, Koganezawa,

and Yamamoto (2019), uses the TakoBot 2 mechanism, which consists of two disks inter-connected by an universal joint and a set of compression springs that increase the robot compliance. The second is the colonoscopy continuum robot by Qi et al. (2023), whose joints are designed with a tenon-mortise system between the segment disks. Additionally, this robot has a helical spring passing through the middle of the disks, forming an elastic backbone, ensuring the continuous deformation of the structure and improving its stiffness.

Compliant joints are commonly used as flexible joints for continuum manipulators and consist of one or more elastic rods that inter-connect disks. Depending on the application, as detailed in the following of this section, these disks can have different shapes. Fig. 9 shows some simple examples of the three most common types of disks extrapolated from the research process: a normal disk, a bevelled disk with the same slope for all the two bevels, and a bevelled disk with a different slope for each bevel. This review revealed that the compliant joints adopted for this kind of robot can be divided between compliant joints, which have just one elastic rod, and twin-pivot compliant joints, which have a pair of elastic rods. Fig. 10 shows the difference between a compliant joint, on the left, and a twin-pivot compliant joint, on the right, where the disks are represented as grey cylinders and the elastic rods composing the joints as black lines. The compliant joint was used in the snake-like arm of the Aircraft Fuel Tank Inspection Robot (AFTIR), presented by Niu, Wang, and Zong (2015). Each AFTIR section comprises a base disk, several support disks, and an end disk, all connected by a flexible backbone that acts as a compliant joint and three driving cables, which provide each segment with two DoF. Differently, the tip section of the bevelled disk-based continuum robot proposed by Wang et al. (2018) and designed for aero-engine repair is composed of twin-pivot compliant joints, one rotated by 90 degrees with respect to the predecessor: this design provides the tip section with two DoF. In the body section, the segments are crossed by a pair of continuous elastic rods that allow the section to bend in just one plane. As in the robot developed by Wang et al. (2021), the bevels of the body section disks have different slopes compared to the tip section. Dong et al. (2017) developed a continuum manipulator to maintain gas turbine engines and divided into base sections and tip sections, both of which have twin-pivot compliant joints in their segments. The twin-pivot compliant joint is designed with standard elastic rods in the base section segments, while, in the tip section segments, composed of bevelled disks, the rods are substituted by lamellae. This design increases the stiffness of the base sections and reduces the dimensions of the tip sections. Twin-pivot compliant joints were adopted also by Dong, Palmer, Axinte, and Kell (2019) for the design of their cable-driven continuum manipulator thought for in-situ repair of maintenance and for the robot presented by Yang, Yang, Sun, and Chen (2023), designed for in-situ aero-engine maintenance. Troncoso et al. (2022) presented another compliant joint form for the active section of the COntinuum roBot for Remote Applications (COBRA), which is a cable-driven multi-backbone robot with pivot disk vertebrae that roll onto each other.

The robot presented by Wang et al. (2021) and thought to maintain aero-engine combustors is composed of a novel twin-pivot revolute joint, which combines compliant and rigid joint characteristics. The manipulator is composed of two parts: a body, with ten 1-DoF sections, and a tip, having three 2-DoF sections. Each section comprises bevelled disks with different angles in the body section with respect to the tip section to obtain the required C-c bending shape. Hence, the robot can enter the small engine access with a small radius of curvature and explore the area exploiting a bigger radius of curvature.

Hong et al. (2018) proposed a continuum robot with ball-and-socket joints and thought to perform maxillary sinus surgery. This concept was later used by the same authors for the distal section of another continuum robot, designed for the same purpose. This latter robot, shown in Hong, Feng, Xie and Yang (2022), comprises a distal section composed of ball-and-socket joints and a proximal section with a novel planar bending joint, developed from the ball-and-socket joint.

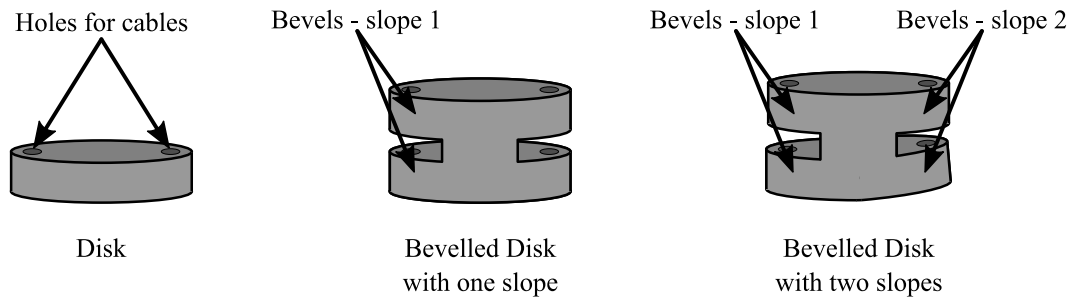


Fig. 9. A scheme of the most commonly used disks for cable-driven continuum manipulators: a flat disk, a bevelled disk with constant slopes among all the bevels, and a bevelled disk with different slopes.

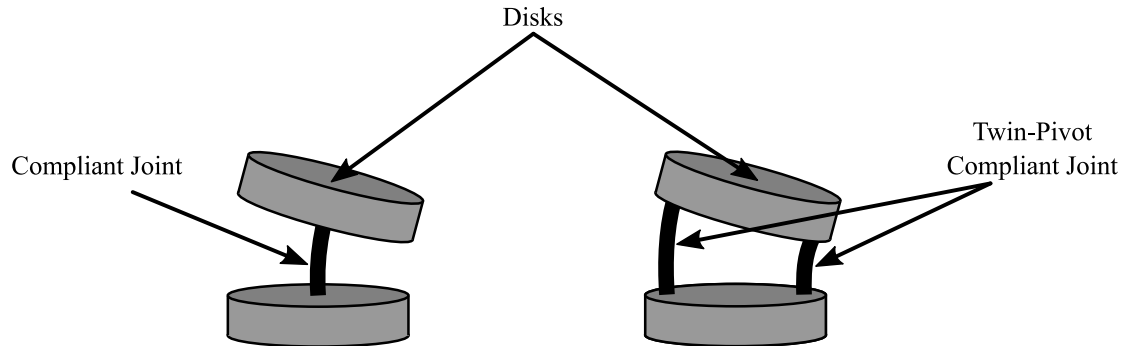


Fig. 10. A scheme of a compliant joint and a twin-pivot compliant joint. The first one is composed by a couple of disks and one elastic rod acting as a joint. The second has a pair of elastic rods connecting the two disks and acting as a joint.

Another continuum manipulator thought for surgery purposes was designed by Wang, Hu, et al. (2023). In particular, the robot is characterised by its small dimensions and by the spring-based structure, which consists of a compression spring in the middle of which there are a NiTi rod, acting as a backbone, and a couple of cables, driving the robot and controlling the end-effector.

Moreover, there exist continuum manipulators whose design is directly inspired by nature. A first example is the continuum robot designed by Amouri, Cherfia, Belkhir, and Merabti (2023), which is inspired by the fish-bone structure and each section of which is composed of a sheet-shaped elastic backbone on which a series of cross-shaped rigid spacer sheet are mounted. The section is driven by an antagonistic couple of inextensible cables passing through the guide holes of the cross-shaped sheet tips, providing each robot section with a planar motion. Another bio-inspired continuum robot is the one proposed by Mavinkurve et al. (2023), which takes its inspiration by the woodpecker extensible tongue mechanism. The design includes a backbone composed of a set of rigid disks interconnected by a NiTi rod and a couple of rods with gears attached to the manipulator tip and free to the other side. The backbone is not directly attached to the motors and the geared rods, engaged with a couple of worm gears attached to the motors, can push and pull the manipulator tip. Consequently, the continuum manipulator backbone can be extended or bend by controlling the length of the two gear rods.

Researchers often emphasise the actuation system of continuum manipulators, especially in cable-driven designs. Indeed, cable actuation can be performed in different ways, depending on the manipulator design and the application requirements. Some examples are the linear lead shaft and the screw nut linear actuators used by Yeshmukhametov et al. (2019) and Yu and Natarajan (2020), respectively, and the rotating motors employed by Dong et al. (2017) and Troncoso et al. (2022). The surgery robot proposed by Hong et al. (2018) is actuated by two rotary motors driving four cables passing in winding pulleys. The actuation system designed for the backbone-driven robot presented by Xu et al. (2014) is composed of an actuation continuum segment

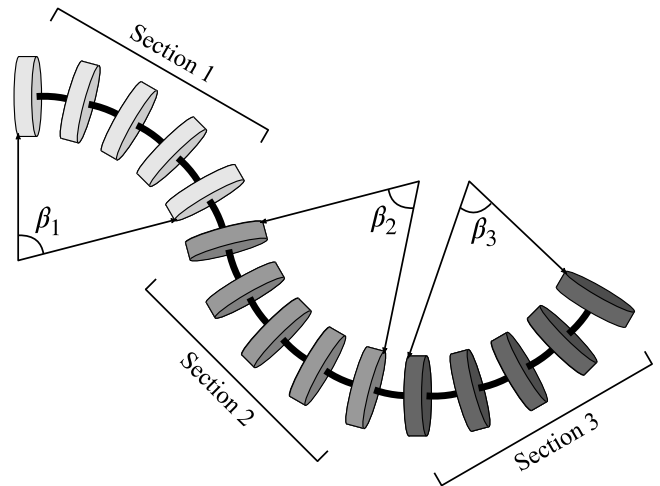


Fig. 11. PCC assumption for a generic continuum manipulator composed of three sections, whose segments are interconnected with compliant joints. The PCC assumption consists in considering each section as a circular arc of angle β_1 , β_2 , and β_3 , respectively.

driven by a motorised ball screw, while the pneumatic growing robot shown by Talas et al. (2020) is equipped with a pinch roller actuator.

4.2. Modelling

To model continuum manipulators kinematics, the Piecewise Constant Curvature (PCC) theory, which is based on the assumption that each section of the continuum manipulator is a circular arc, is widely employed. Fig. 11 represents a schema of the PCC assumption, in which Section 1, Section 2, and Section 3 are modelled as if they were circular arcs with angles β_1 , β_2 , and β_3 , respectively. Wang et al. (2018) developed a continuum manipulator to repair aero-engines and

exploited the PCC method to model its kinematics, implementing both the task-configuration and the configuration-actuation space maps. Furthermore, the authors also implemented the configuration-cable kinematic map, calculating the length of the cables with respect to the bending arc configuration in each manipulator section. The forward kinematics of the maxillary sinus surgery robot proposed by Hong et al. (2018) is described using the PCC theory and the DH method, described by Jones and Walker (2006). Yu and Natarajan (2020) proposed a probabilistic approach to model a continuum manipulator, in which the kinematic model is learnt from experimental data sets produced using a PCC-based open-loop position controller. It is then used to train a Dynamic Gaussian Mixture Model (DGMM), which captures the relationship between the actuator and task space of the continuum robot. It was trained with 6000 samples. Wang et al. (2021) established a new PCC-based kinematic model for a continuum manipulator designed with a combination of rigid and compliant joints. This model, called Segment-PCC, decomposes each section of the continuum manipulator into multiple segments that represent units of curvature and uses the static model of the robot, produced using the Kirchhoff elastic rod theory, to calculate the different bending angles in segments. Later, Hong, Zhou, et al. (2022) proposed a new continuum manipulator for maxillary sinus surgery and produced a homogeneous transformation-based forward kinematics and a Jacobian-based inverse kinematic model starting from the PCC assumption. Troncoso et al. (2022) employed a similar approach for the COBRA system. Hong, Feng, et al. (2022) developed a kinematic model of their continuum robot for maxillary sinus surgery using the variable curvature continuum kinematics method, described by Mahl, Hildebrandt, and Sawodny (2014), and applying the PCC method to some segments of the robot. Recently, also Mavinkurve et al. (2023) exploited the PCC assumption to model the continuum manipulator inspired by the woodpecker tongue, as well as Yang et al. (2023), who proposed a kinetostatic model of the continuum manipulator thought for aero-engine maintenance.

Although the PCC assumption is acceptable for short continuum robots, for which the inaccuracy of the model can be considered negligible, Ba et al. (2021) demonstrated how it introduces a non-negligible mismatch between the actual shape of the manipulator section and the circular arc in longer manipulators. Hence, to produce the task-configuration map of a continuum manipulator, they used homogeneous transformations without applying the PCC assumption. Homogeneous transformation is a commonly adopted tool to describe the kinematics of both DJHRMs and continuum manipulators. Indeed, Xu et al. (2014), used homogeneous transformations to describe the kinematics of a multi-backbone continuum manipulator, exploited to perform the structure synthesis of the robot. Another example is AFTIR, whose kinematic model proposed by Niu et al. (2015) is evaluated via homogeneous transformations of its sections. Similarly, Yeshmukhametov et al. (2019) used homogeneous transformations to model the forward kinematics of their continuum robot designed with universal joints and coil compression springs. Cobos-Guzman, Palmer, and Axinte (2017) developed a continuum robot composed of compliant joints and used homogeneous transformations and Euler angles to calculate the kinematic model of the manipulator, including a logic structure able to avoid kinematic singularities. A similar logic structure is also applied in the inverse kinematics solution, which is calculated via a novel approach to evaluate the Jacobian matrix. Homogeneous transformations are also exploited by Seleem, El-Hussieny, and Assal (2018) and Qi et al. (2023). The former modelled continuum robots' forward kinematics and Jacobian-based differential kinematics. The latter employed the DH method to calculate the transformations used to evaluate the kinematic model of an endoscopy continuum robot. Similarly, Amouri et al. (2023) modelled the kinematics of their fish-backbone-inspired continuum manipulator using homogeneous transformations.

Further, Dong et al. (2017) performed a geometric analysis of a cable kinematics of the continuum robot composed of compliant joints. The kinematics of the cable-driven continuum robot proposed by Dong

et al. (2019) and composed of twin-pivot compliant joints was modelled considering the displacement due to the cables slack, while the kinematic model of the waterjet-actuated soft robot HydroJet presented by Campisano, Ramirez, Caló, et al. (2020) used both the Crosserat rod theory and the Pseudo-Rigid Body kinematics. Finally, by Mu, Chen, Li, Qian, and Ding (2021) used the Spatial Biarc method to model the kinematics of concentric cable-driven continuum manipulators.

As already mentioned, kinematic modelling of continuum manipulators is one of the key research field. Nevertheless, a couple of studies dealing with the dynamic model of this kind of robots were identified during the review procedure. Xu and He (2022) and Sofla, Sadigh, Sadati, Bergeles, and Zareinejad (2023), indeed, modelled two different continuum robots using the canonical Lagrange's formulation of the equation of motion.

4.3. Control

The control of continuum manipulators is a complex problem due to many factors, like the intrinsic hyper-redundancy, the uncertainties introduced by the actuation system, the difficulty of integrating sensors into the often very small and flexible structure and producing a precise robot model. However, the review described in Section 2 shows that different control strategies, both open-loop and closed-loop, are possible and these can increase the motion precision and accuracy of continuum manipulators. Fig. 12 shows a simple representation of a generic open-loop control scheme, reported on the left side of the picture, and a generic closed-loop control scheme, depicted on the right side of the picture, and highlights the difference between the two approaches, which consists in the presence of a feedback in closed-loop control scheme that is absent in the open-loop one.

Kinematic control of robotic arms is often faced by solving the inverse kinematic problem using the pseudo-inverse of the Jacobian matrix. Yeshmukhametov et al. (2019) applied this strategy to control a continuum robot composed of universal joints as well as Wang, Hu, et al. (2023) did for their miniature spring-based continuum manipulator, while Cobos-Guzman et al. (2017) devised a novel singularity-free approach to evaluate the Jacobian matrix. However, given the intrinsic hyper-redundancy of continuum manipulators, the inverse kinematic problem for these kind of robots has multiple solutions. For this reason, Wu, Yu, Pan, Li, and Pei (2022) designed the Continuum Robot Reaching Inverse Kinematics algorithm, which is a heuristic algorithm inspired by the FABRIK method that has a high convergence rate and low computational cost, and Wild et al. (2024) presented the Piecewise Dual Quaternion algorithm, which selects the optimal solution of the problem respecting the constraints and minimising a cost function performing iterative nonlinear optimisation.

Nevertheless, this review shows that the most common approach to determining the motion of continuum manipulators is the tip-following approach, which is a variation of the follow-the-leader approach presented in Section 3.3 and depicted in Fig. 8(a). In the context of continuum manipulators, the algorithm is called tip-following because it works at section level, meaning that it forces all the robot sections to trace the trajectory of the tip section. This strategy overcomes the problem of kinematic hyper-redundancy. The tip-following approach was employed by Dong et al. (2017) to control the motion of a compliant joint-based continuum manipulator, by Wang et al. (2018) to allow a bevelled disk-based robot to perform the required C-c shape motion, by Troncoso et al. (2022) to control the active segment of a teleoperated manipulator composed by pivot disk vertebrae, and by Hong, Zhou, et al. (2022) for the kinematic control of a flexible endoscope.

Although tip-following is the most widespread strategy, other approaches have been developed. Guochen, Li, Qingji, and Dandan (2014) designed a path-tracking algorithm that decomposes the trajectory into several segments that must be sequentially tracked by each segment of the robot. This algorithm exploits the PCC assumption. Seleem et al. (2018) implemented a motion planning framework that starts from a

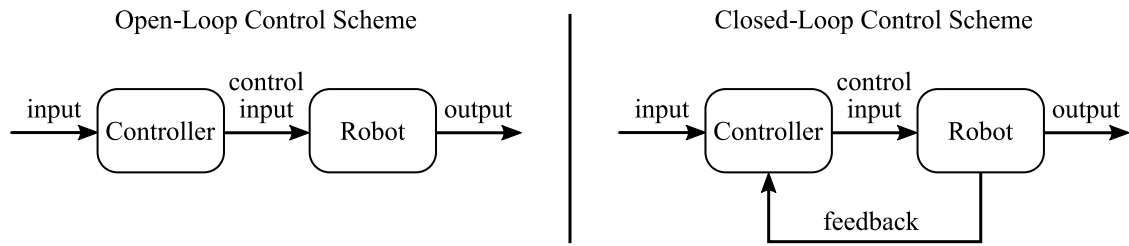


Fig. 12. Generic open-loop controller, on the left, and closed-loop controller, on the right. The difference between the two approaches consists in the feedback, which is present in the closed-loop control and absent in the open-loop one.

human demonstration. A physical flexible interface, equipped with an Inertial Measurement Unit (IMU), is provided to the operator, who performs some demonstrations that the robot must reproduce. The inverse kinematics of the continuum manipulator is solved through the pseudo-inverse of the Jacobian matrix. Qi et al. (2023) proposed a motion planning method for multi-segment flexible continuum manipulators based on the backbone cure method, which is equivalent to finding the optimal solution of the inverse kinematics when the obstacles and path are known. The experimental campaign is conducted using a controller-responder control system.

In general, open-loop controllers rely on the inverse kinematics of the robot. However, since there is often a discrepancy between the real shape and the kinematic model of a continuum robot, some precautions must be taken. Hence, Liu, Yang, et al. (2016) implemented an actuation compensation given in feed-forward to a compliant joint-based continuum manipulator that increases its performance. Other examples are the open-loop position and speed controllers that Talas et al. (2020) developed to control the tip of their teleoperated growing pneumatic soft robot. Their results showed that the position controller is negatively affected by the growth of the robot backbone and that the kinematic model is not precise enough to apply that controller when the robot is moving in constrained environments. However, the speed controller position error is mainly due to gravity and can be reduced by decreasing the end-effector weight. Yu and Natarajan (2020) proposed a controller based on the DGMM, using the kinematic model described in Section 4.2. An open-loop PCC-based controller was implemented and compared to the DGMM-based controller in a trajectory tracking experiment, in which the DGMM-based controller showed significant improvement compared to the PCC-based controller. To compensate for changes in cable length during the motion of a cable-driven continuum manipulator, Hong, Feng, et al. (2022) proposed a motion compensation method to eliminate coupling effect. This compensation was combined with a compensation of the cable tension, obtained considering the cable as a flexible Euler-Bernoulli beam, for which force feedback is required.

Except for this cable tension compensation, all the previous approaches are open-loop, but this review revealed that closed-loop control is also possible. Niu et al. (2015) developed a fuzzy-logic controller based on attitude feedback for a cable-driven continuum robot with flexible backbones. The controller input is the maximum cable length deviation, evaluated with the kinematic model of the robot, and its time derivative. Through a set of fuzzy rules, the controller outputs the driving cable velocity. The performance of this controller was compared with a PID controller in experiments that showed that the fuzzy-logic controller provides a decrease in overshoot and transient time constant. Seleem et al. (2018) combined their human demonstration-based kinematic control strategy with an adaptation mechanism designed to overcome possible external disturbances and model uncertainties. This strategy, called Model Reference Adaptive Control, evaluates a gain matrix, which results from the integral of the norm of the state error multiplied by a rate of adaptation, that the kinematic controller uses to avoid possible drifting during the trajectory tracking. Campisano, Ramirez, Landewee, et al. (2020) implemented a contact detection system as an anti-windup method in the PID controller applied to

HydroJet. The robot is teleoperated using a thumb-controller joystick, whose output is given as input to a quasi-static motion controller including the PID controller, the Crosserod Rod model of the robot mentioned in Section 4.2, and a redundancy optimisation block. This controller produces the desired robot configuration as its output. Another fuzzy-logic controller was developed by Ba et al. (2021) to address the challenges of the PCC assumption mismatch for the same robot presented by Wang et al. (2021). This controller consists of two independent fuzzy controllers, one for the radial positioning error and one for the angular positioning error at the robot tip. The overall controller takes as its input the desired tip position and its actual position, measured by a motion capture system, and produces as its output the displacement of the cables, which is used to correct the length of the cables given by the kinematic model. A comparison is made with a PCC-based controller, highlighting how the fuzzy-logic controller can overcome the PCC assumption mismatch, which, in some testing points, prevented the PCC-based controller from converging. To ensure the motion controllability of a cable-driven continuum manipulator, Troncoso et al. (2022) developed a closed-loop controller with tension feedback given by load cells. This controller aims to maintain tension in antagonistic cable pairs, preventing cables from falling off pulleys, while Fang, Dong, Mohammad, and Axinte (2023) implemented a two-level closed-loop controller based on the feedback given by a hybrid sensing system to control the same robot proposed by Dong et al. (2019).

Regarding the dynamic control of continuum manipulators, Xu and He (2022) defined an adaptive control law using the function approximation technique to reject possible inaccuracy in the model or external unknown disturbances. For the same reason, Sofla et al. (2023) designed a sliding mode controller with variable gain that ensures the asymptotic stability of the closed-loop system.

5. Mobile manipulators

Mobile manipulators are single or multiple robotic arms attached to mobile platforms, which can be either terrestrial, aerial, or submarine. Generically, a mobile platform is free to move in space relative to a fixed frame. Such motion is known as floating base and it is represented by a 6-DoF joint, as described by Siciliano and Khatib (2016). A mobile manipulator combines 6-DoF floating base with an arm having an arbitrary number of DoF. Therefore, almost all of mobile manipulators are redundant or hyper-redundant systems and have a wider workspace than fixed manipulators. In terms of modelling, mobile manipulators are described by un-actuated variables and actuated joint variables.

Since the floating base is not directly actuated, the motion of the system can only be modified by applying external forces to the environment. Mobile manipulators can have very different architectures in terms of locomotion, as shown in Fig. 13. Some ground platforms are equipped with wheels, tracks, or legs. Hybrid platforms result from the combination of legs and wheels. Further, some ground platforms, such as snake robots, resort to interactions between their bodies and the ground. Unmanned Aerial Vehicles (UAVs), Autonomous Underwater Vehicles (AUVs), and Remotely Operated Vehicles (ROVs) make use of propellers, impellers or thrusters to navigate in the environment.

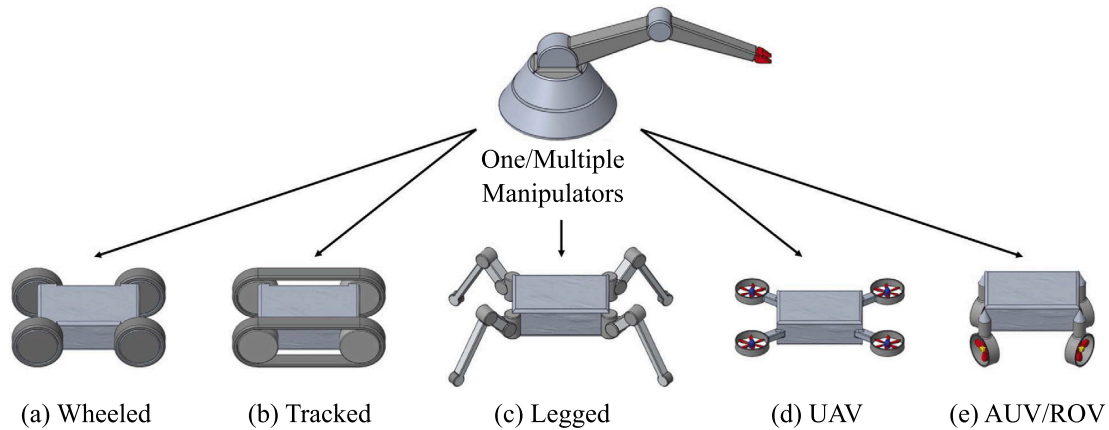


Fig. 13. Representation of common locomotion typologies in mobile manipulators: (a) Wheeled vehicle; (b) Tracked vehicle; (c) Legged platform; (d) Unmanned Aerial Vehicle (UAV); (e) Autonomous Underwater Vehicle (AUV)/ Remotely Operated Vehicle. Mobile platforms can equip one or multiple manipulators.

In terms of control, mobile manipulators present a wide set of challenges. Firstly, these systems require sensors and sensor fusion algorithms to allow localisation and navigation. Control laws and path-planning algorithms are needed to effectively move the mobile platform toward the desired position. Also the manipulators require specific control laws to perform the desired actions. In some cases, whole-body controllers are defined to better coordinate the mobile platform with the arm motion and to achieve a more precise positioning of the end-effector. Finally, teleoperation interfaces can be developed to enable single or multiple operators remote control applications. Generally, mobile manipulators have been deployed in all scenarios that pose a threat to human life such as search and rescue, emergency response, space and planetary explorations. The combination of spatial mobility and manipulation ability makes mobile manipulators particularly suitable for inspection and maintenance operations in oil and gas, nuclear, civil, and industrial infrastructures.

This section studies the main features and challenges of the mobile manipulators found in the literature. Section 5.1 describes the designs developed. Section 5.2 discusses the modelling technique adopted. Section 5.3 provides an overview of control techniques and teleoperation interfaces developed for mobile manipulators. Most of the selected documents focus on ground platforms (68 %). UAVs are addressed in four documents (16 %), three of which are recent reviews compiled by Ruggiero, Lippiello, and Ollero (2018), Khamseh, Janabi-Sharifi, and Abdessameud (2018), and Ollero, Tognon, Suarez, Lee, and Franchi (2021). AUVs and ROVs manipulators are described in four documents (16 %).

5.1. Design

Mobile manipulators have very different morphology and features depending on their target applications and operating environment. In most instances, especially for ground platforms, the primary focus is the platform design and the locomotion system.

For example, inspections in underground tunnels at the European Organization for Nuclear Research (CERN) pose multiple challenges and create strict requirements. In this context, Prados Sesmero, Buonocore, and Di Castro (2021) proposed a novel omnidirectional wheeled platform. The wheels are located in a rectangle with straight forward orientation and this layout makes the system redundant. This platform has four actuated DoF, while the floating base has only three acDoF, two translations and one rotation. The platform is equipped with the off-the-shelf robotic arm Jaco by Kinova. The manipulator brings a radiation sensor to a target location during radiation surveys and delivers task-specific tools in other cases.

Kim, Jung, and Kim (1999) designed the KAEROT/m2 for inspection of pressure tubes in the Primary Heat Transport System (PHTS) of the Pressurised Heavy Water Reactor (PHWR). This mobile manipulator consists of a long-reach mast and re-configurable tracked platform. The mast carries a surveillance camera that can move up and down from 1.7 m to 9.3 m allowing the operator to inspect the environment. Buckingham and Graham (2012) developed the SAFIRE robot to inspect primary circuit pipework, feeder pipes, and header tanks in the CANada Deuterium Uranium (CANDU) reactors. SAFIRE is a remotely controlled mobile manipulator equipped with a 18-DoF snake-arm. This manipulator can snake under catwalks and between hangers to take images of the pipework. Due to the limited space in walkways, the arm can be wrapped around the actuator pack and mounted on a tracked vehicle. Hilaro et al. (2019) designed a mobile manipulator for inspection in industrial plants, with the goal of monitoring the readings of analog gauges. This modular platform can perform accurate visual inspections. Design constraints were imposed on the dimensions, speed and weight, slopes and stairs negotiation, and valves handling abilities. During the design phase, the static free body diagram of this system was used to assess the required torques. The mobile platform consists of four parts: the main body, flippers for stairs negotiation, a custom robotic arm, and a gripper as end-effector. For mining plants, the robot ROSI was developed for inspections of belt conveyors by Rocha et al. (2021). They developed a wheeled-tracked platform with flippers and with an embedded robotic arm. Due to the harsh environment ROSI experiences, the platform's main body has an adequate sealing to prevent water and dust ingress. For the same reason, the traction systems are embedded into the main body. The embedded manipulator is an off-the-shelf solution: the 7-DoF Kinova Robotics Gen3.

During the DARPA Robotic Challenge (DRC), many systems were developed to accomplish very demanding inspection and maintenance operations in dangerous, degraded, human-engineered environments. RoboSimian, developed at JPL by Hebert et al. (2015), was designed to fit into and through confined spaces. RoboSimian has four general-purpose limbs capable of both mobility and manipulation arranged in an axisymmetric fashion. RoboSimian also has two active wheels on its body, and two passive wheels on the 7-DoF limbs driven by lightweight, high-torque actuators. Each limb has a six-axis force/torque sensor supporting the end-effectors. Each hand has three under-actuated fingers. The closing order of the fingers is tuned via pulley diameter and return springs. Another platform that competed at the DRC was the Momaro, developed by Schwarz et al. (2017). Momaro was mainly designed for addressing disaster scenarios such as the Fukushima nuclear accident. Momaro has four articulated compliant legs that end in pairs of directly driven, steerable wheels. This unique base design combines advantages of driving and stepping locomotion. The legs have three pitch joints

in the hip, knee, and ankle, allowing the adjustment of the wheel pair position relative to the trunk. The ankle can rotate around the yaw axis. To perform a wide range of manipulation tasks, Momaro has an anthropomorphic upper body connected by a yaw joint to the base and with two 7-DoF manipulators that end in dexterous hands equipped with four 2-DoF fingers. Building on the DRC designs, Klamt et al. (2020) developed the Centauro robot. Centauro was designed to provide mobile manipulation in construction and maintenance of manned and unmanned stations, as well as exploration of planetary environments. The system was evaluated at the facilities of Kerntechnische Hilfsdienst GmbH (KHG), which is part of the German Nuclear Emergency Response Organisation. The lower body consists of four 5-DoF legs in a spider-like configuration. Each hip module consists of a yaw and a pitch joint, followed by another pitch joint in the knee. Each ankle has a pitch and a yaw joint which allows for steering of the wheel. The robot torso is equipped with two 7-DoF arms and an additional rotational joint in the waist. The two arms have different end-effectors: a compliant, robust 1-DoF SoftHand and an anthropomorphic Schunk hand with nine DoF. Overall, the Centauro robot has 52 DoF.

Differently from the solely above-mentioned electric-actuated robots, Gong et al. (2019, 2021) attached a pneumatic soft manipulator to a small ROV with four DoF. The underwater soft manipulator consists of four sections: two bending segments, one elongation segment, and one soft gripper. The bending and elongation segments have a circular cross-section to decrease the hydrodynamic resistance in the water. Bending segments have three individual chambers covered with rubber tendons to reduce the ballooning. Fibre-reinforced actuators on the elongation segments provide extension in the vertical direction while grasping underwater. This system was designed for collecting seafood animals cultivated in shallow waters. A similar design was adopted by Phillips et al. (2018). Here, the soft manipulator and the gripper were designed for deep-sea sampling. The multi-DoF arm consists of modular bending, twisting, and gripping modules, which are powered using low-pressure seawater drawn from the surrounding environment.

5.2. Modelling

Defining kinematic and dynamic models of mobile manipulators is not a trivial task, because the floating base DoF are combined with the DoF of the overall system. Additionally, when mobile platforms have wheels or tracks, kinematic constraints have to be established to relate the floating base velocity to wheel or track velocities. For dynamic models of mobile manipulators, the external forces that affect the position and orientation of the mobile platform must be considered. Moreover, dynamic models have to comply with the kinematic constraints to ensure a coherent system behaviour. Among the selected documents in this literature review, only a few describe the method used for defining the kinematic and dynamic models in detail. However, in most of the documents such models are used for developing control laws and path-planning algorithms, as stated by Klamt et al. (2020) and Yan et al. (2020).

Hebert et al. (2015) devoted a node of the software architecture to the robot modelling. The so called *modelling module* is responsible for maintaining and sharing kinematic, geometric, and other physical properties of the robot, objects, and environment with the other nodes. Using the model data structure and current state of the system, generic functions compute the forward kinematics, Jacobians, centre-of-mass, and collisions. The *modelling module* allows drawing the RoboSimian actual configuration with OpenGL for the visualisation in operator interfaces. Specialised algorithms are used for closed-form inverse kinematics of the RoboSimian limbs, with multiple approaches for redundancy resolution. Rocha et al. (2021) designed the ROSI platform, a wheeled-tracked system whose kinematics is constrained in the horizontal plane. The floating base is provided with three DoF: the longitudinal and later translations and the yaw rotation, which represents the vehicle orientation. The authors assumed that the platform is

a differential robot with forward and steering velocities, and remapped the omnidirectional floating base velocity to the wheels angular velocities using kinematic constraints. Finally, the relationship between the joint velocities and the end-effector linear and angular velocities was established using the geometric Jacobian of the system. Gong et al. (2019, 2021) detailed the algorithms for computing the forward and inverse kinematics in their underwater soft manipulator. By design, the two bending segments of the manipulator are actuated with the same bending curvature but opposite bending directions. In addition, the authors assumed a linear relationship for the pressures in the opposing chambers of each soft segment. In modelling the manipulator's forward kinematics, the authors assumed that the bending sections have a constant curvature rate and that the curves are tangent at the intersection point. They also assumed that the chambers within the same segment are parallel with equal cross sections. Using this method, the authors achieved coordinate based control allowing point-to-point movements of the soft manipulator. Their rapid inverse kinematic solution is based on the constraint that at most two chambers in a bending segment are actuated simultaneously, so that at least one chamber of the bent segment is in its initial length.

A thorough analysis on how crucial the dynamic control is for coordinated motion of mobile manipulators was performed by Holmberg and Khatib (2000). They noted that the equations of motion of mobile manipulators are typically formed in two ways: by deriving the whole-body dynamics and applying the constraints or by splitting the system into pieces, solving the dynamics and using loop closure equations. They, however, modelled the mobile platform as a collection of open-chain manipulators. Each open-chain wheel consists of steer, roll, and twist variables. Because of the nature of the final mechanism, they defined the relationship between wheel module speeds and local Cartesian speeds. They derived the operational space dynamics of each manipulator, then, the overall operational space dynamics of the mobile base was obtained by using the augmented object model. Prados Sesmero et al. (2021) described the platform kinematics in the ground plane. The inertial reference system is defined and local frames are located on the body, wheels, and mecanum rollers. As for most wheeled robots, the floating base is described by the longitudinal and later translations and the vehicle orientation. Once the platform velocity vector was determined, the authors defined the kinematics constraints of the mecanum wheels. Projecting the robot kinematics on the constraints, they obtained the map between the wheels velocities and the platform motion. For the dynamic model, they defined the equation of motion adopting the Lagrangian approach and modelled the robot dynamics in the operational space variables.

In the field of UAVs, the mobile platform vibrations degrade the accuracy of gyroscope and accelerometer measurements used for flight stability, as well as the image quality of onboard vision systems. Cocuzza and Doria (2021) carried out the vibrations analysis of a heavy payload octocopter using Experimental Modal Analysis (EMA). They proposed a simplified Mass-Spring-Damper (MSD) dynamic model of the system, whose dynamic parameters are identified by analysing the experimental modes of vibration. The first mode of vibration involves the main platform and the suspended mass, i.e. the manipulator, while the second involves the main platform and the motors. Consequently, a 1-DoF model was defined to identify the damping and stiffness parameters of the first mode, and a 2-DoF model for the parameters identification of the second mode. The final 3-DoF MSD model combines the motions of the motors, the main platform, and the manipulator. Combining the identified parameters, the model eigenfrequencies were computed and the error with respect to the experimental ones was less than 1.5%.

5.3. Control

Designing effective control strategies for accomplishing inspection missions in hazardous environments using mobile manipulators represents a big challenge. Kinematic or dynamic based controllers have to

operate in combination with path or trajectory planners and perception systems to generate safe and feasible control input for the robot. Highly dynamic environments, complex tasks, and unpredictable scenarios often require the robot to be supervised or teleoperated by skilled operators. The design of an immersive and intuitive human–robot interfaces necessitates trade-off solutions between easy operability, situational awareness, and cognitive load to facilitate the operator in making decisions, controlling the robot, and accomplishing the mission. The selected documents about mobile manipulators cover these topics from different perspectives. Some of them focus on the robot control from a theoretical point of view proposing effective control strategies. Others adopt a more practical approach and propose hierarchical control architectures, control nodes, planner and perception modules together with teleoperation interfaces. Some contributions, instead, directly address the open challenges in teleoperation, such as the communication delays or the multi-user operability, and propose innovative solutions.

5.3.1. Robot control

Among the documents selected in this literature review, only two of these addressed the robot control from a theoretical point of view. Holmberg and Khatib (2000) described the dynamic decoupling control for a wheeled mobile manipulator, achieved by selecting the operational space control structure. In this approach, the authors defined the relationship between the observed robot joint speeds and the operational speeds of each wheel as a constraint matrix. The overall motion of the joints in the robot is described by gathering all the wheel constraint matrices. Applying this dynamic decoupled control, the effort is spread as evenly as possible among the wheels and the tendency for each wheel to lose traction is reduced. The experimental results show full dynamic decoupling and improved performance in controlling the mobile manipulator. Sharma, Singh, Vanualailai, and Prasad (2018) noted that the problem of motion planning and formation control of a globally rigid formation of nonholonomic vehicles represents an open problem. The authors proposed a formation control of a team of doubly nonholonomic mobile manipulators by using an integration of the Lyapunov-based Control Scheme (LbCS) and the leader–follower scheme containing a virtual leader. Based on the LbCS, the proposed motion planner guarantees the establishment of a globally rigid formation. For moving the formation, the authors assigned a virtual leader to the team of mobile manipulators.

The remainder of the selected documents describe more practical approaches to control mobile manipulators. The control of RoboSimian behaviour was performed onboard the robot by combining a *mobile manipulation motion* planner and a *behaviour* planner, as designed by Hebert et al. (2015). The mobile manipulation motion planning ensures that the robot remains statically stable at all times, and that all motions are kinematically feasible, smooth, and collision-free. The authors proposed the decomposition of the mobile manipulation planning problem into a combination of open-chain and closed-chain motion planning problems. The open-chain planner is responsible for the motions of an unconstrained serial manipulator system in joint space. The closed-chain planner addresses the motion of a parallel manipulator system in Cartesian space of the manipulator base frame. The *behaviour* planner, whose output is a set of desired body poses and joint angles, is used to generate the motion specifications. For each pose, the *behaviour* planner determines if there is an inverse kinematic solution for the desired pose. For mobility behaviours, such as walking, climbing, or shifting the body, the *behaviour* planner is responsible for producing a set of body and end-effector poses, and an inverse kinematic reference posture, which is then fed to the motion planner.

The Momaro robot, designed by Schwarz et al. (2017), is controlled through a kinematic controller, in which all limbs and the torso yaw joint are considered separately. The Cartesian goal configuration for a limb is defined through telemanipulation or dedicated motion primitives. Interpolated Cartesian poses are converted to joint space positions via inverse kinematics. Finally, the desired robot configuration

is checked for self-collisions and, if collision-free, fed to the low-level hardware controllers for execution. For the 7-DoF arms, the authors calculated the inverse kinematics with redundancy resolution using the selectively damped-least squares approach. For the legs, the inverse kinematic problem is solved with a custom analytical kinematics solver. For driving the omnidirectional platform, the operator can control the locomotion using a joystick, which generated velocity commands. While driving, the robot controls the orientation of each ankle using IMU information to keep the ankle vertical with respect to the ground. Also in this case, the operator retains control of the platform linear velocity using a joystick during semi-autonomous stepping.

For the Centauro robot, Klamt et al. (2020) implemented a real-time Cartesian control and a hierarchical whole-body control. For environment perception, ground contact estimations are made via forward dynamics that produce a 6D force vector for each foot. Whenever the force exerted by the foot exceeds a threshold, a contact is detected. Laser-based 3D mapping of the environment helps in localisation of the Centauro robot. To enable autonomous or semi-autonomous manipulation, the Centauro robot determines the pose of useful objects in its environment using Convolutional Neural Network (CNN) models. For pose estimation on a rough scale, the authors developed a 5D pose predictor network. Autonomous locomotion planning and execution are used to increase locomotion speed and stability, to lower the cognitive load on operators, and to plan locomotion under bad data transmission.

Based on the whole-body model described in Section 5.2, Rocha et al. (2021) proposed a control law for the ROSI platform. The end-effector actual position is driven to the desired one by using joint velocities. These variables are obtained using the damped least-squares inverse method applied to the geometric Jacobian, which is defined in the whole-body model. For controlling the manipulator, the authors proposed a control scheme for regulating the contact force with a given surface. Basic position and velocity control strategies are used in approaching the surface, then, the control switched to force regulation for providing compliance to the system. For stairs negotiation, the authors designed a semi-automatic climbing algorithm that alleviate the cognitive load of the operator, which is responsible of controlling only the robot linear velocity.

For controlling the mobile manipulator, Prados Sesmero et al. (2021) proposed a hierarchical control architecture divided in two levels: the *Decisional*, and the *Executive* level. At the *Decisional* level there are the following three nodes: the Graphical User Interface (GUI) node, the Supervisor node, and the Task Manager node. Through the GUI, the user can control the robot setting goals and tasks, observe its status, and visualise the information from the sensors. The Supervisor node is responsible for observing the robot status and taking decisions in case of internal errors. The Task Manager node is a finite state machine responsible for the main objective division into small tasks. At *Executive* level there are the following five nodes: the Hardware node, the Motor Controller node, the Robot Model node, the Path planner node, and the SLAM node. The Hardware node consists of motors and drivers. The Motor Controller node controls the motors according to desired positions and velocities. The Robot Model node includes the mobile manipulator models. The Path planner node generates the trajectory for achieving the goal task. The SLAM node is responsible for the simultaneous location and mapping of the environment.

5.3.2. Teleoperation

Nowadays, available mobile manipulators lack in providing that level of usability for being extensively employed in real case scenarios. Additionally, mobile manipulators often require a pool of skilled operators to successfully accomplish missions in hazardous environments. Certain tasks may even require a certain degree of synchronisation between team of robots, which is not trivial to achieve when multiple operators are involved.

As shown in Fig. 14, teleoperation can be divided in three main areas: perception interfaces, situational awareness and user inputs. All

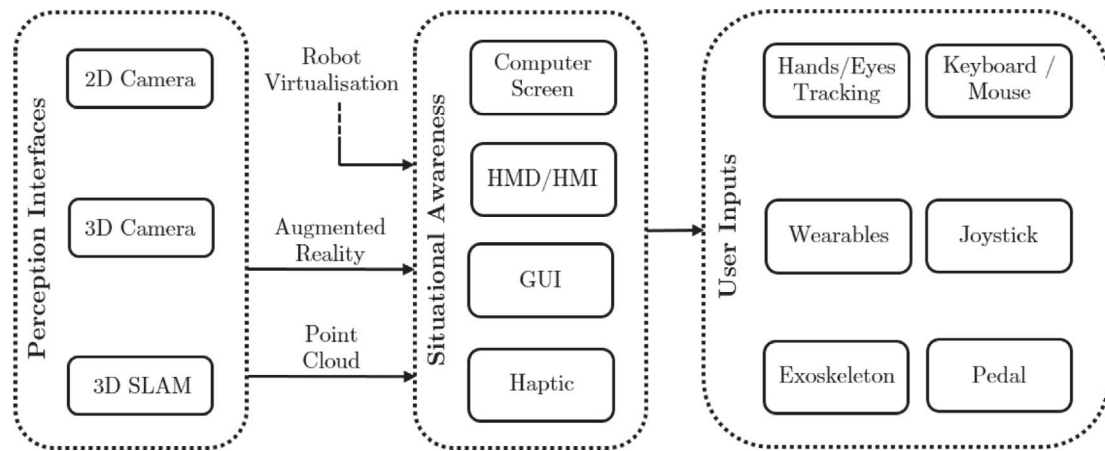


Fig. 14. Teleoperation architecture. The Perception Interfaces block includes the sensing instruments. Augmented Reality, Point Cloud, and Robot Virtualisation provide the operator with crucial information for guiding the robot. The Situational Awareness block comprises technologies that make the operator informed about the robot status. The User Inputs block contains devices to directly control the robot.

devices capable of sensing the environment where the robot is belong to the perception interfaces area. Combining visual feedback from 2D/3D cameras with 3D SLAM information into augmented reality or point clouds provides the operator with situational awareness about the robot status and the surrounding environment. Computer screens, Head Mounted Devices (HMD), Human Machine Interfaces (HMI), Graphical User Interfaces, and Haptic devices help the operator in gaining situational awareness and in decision-making. Finally, the user input devices allow to control the mobile manipulator and accomplish the task.

Concerning situational awareness, [Su, Chen, Zhou, Pretty, and Chase \(2022\)](#) investigated the importance of user perception and spatial awareness of the remote environment when remotely guiding complex robotic systems. Two MR integrated 3D/2D vision and motion mapping frameworks are proposed. In the MR-3D stereoscopic vision (MR-3DSV), the binocular camera stereoscopic view is complemented by two monocular RGB cameras that provide 2D perspectives from the robot wrist and workspace. In the MR-3D point cloud (MR-3DPC), the two monocular RGB cameras augment the live stream of the 3D point cloud. Non-skilled operators were asked to perform pick-and-place, assembly, and dexterous manufacturing tasks using the mobile manipulator platform, which consisted of a 6-DoF industrial manipulator, a 3D-printed parallel gripper, and a mobile base. Both the MR-3DSV and MR-3DPC methods assist teleoperation by reducing the training phase, the task completion time, and the cognitive workload. In terms of continuity in the user control actions, the results indicate that the MR-3DPC framework outperformed the MR-3DSV method.

Concerning easy operability, [Cruz Ulloa, Domínguez, Del Cerro, and Barrientos \(2022\)](#) proposed a MR teleoperation method for high-level control of a 6-DoF arm manipulator integrated on the quadruped robot ARTU-R by Unitree to perform manipulation tasks in search and rescue environments. By wearing the holographic device Hololens, the robot operator is provided with enhanced situation awareness through the virtual robot projection on the real work. In the Hololens environment, the operator can drag through gestures a blue sphere attached to the manipulator end-effector providing high-level commands to the mobile manipulator. The desired trajectory is verified by the collision free planner and then executed by the real system. The control performance obtained with the proposed method are compared against the use of conventional interfaces, i.e. those based on a single or multiple screens, mouse, and keyboard. The results show that the MR interface outperforms conventional interfaces after a series of training sessions, especially for more complex tasks that require object manipulation. For perception, the RoboSimian robot proposed by [Hebert et al. \(2015\)](#) has a system responsible for building, maintaining, and processing 3D maps based on the stereo range images and the visual odometry poses,

which are computed by the camera module. The remote module is designed to control the robot and to model the world. The remote-interface allows configuring the robot's "end-state" and requesting a planned solution to move all the limbs and joints to properly end in that configuration via key-presses and mouse clicks. Such an interface also allows for inserting known models of objects (e.g., valves, ladders, hoses, etc.) into the world manually, so that RoboSimian could interact with objects for manipulation. Due to bandwidth limitations, semi-autonomous behaviours are developed to allow the user to specify any chained sequence of behaviours to follow.

[Schwarz et al. \(2017\)](#) designed the Momaro robot to be controllable by using just two operators, however the actual operators are seven. Operator situational awareness is gained through 3D environment visualisation and transmitted camera images. A set of motion editing tools are developed to support the operators in creating new robot motions. At runtime, these motions could be modified, loaded and finally executed by the robot. For intuitive and flexible manipulation, an operator is designated to control the robot. To do this, the operator wear an head-mounted device, which displays an egocentric view from the perspective of the robot. The operator head is tracked in six DoF motion. These movements are used to update the stereoscopic view of the robot and to allow the operator to freely look around in the current scene. The measured position and orientation of the operator hands are mapped to the position and orientation of the respective gripper of the robot. During driving locomotion, the mobile platform velocity is controlled using a 4-axis joystick. The operator is able to control the robot footprints and the platform attitude using a custom base control GUI.

In oil and gas applications, [Garcia et al. \(2018\)](#) pointed out that teleoperation control schemes need to ensure real-time execution of commands. The authors presented a flexible robotic teleoperation architecture for multipurpose industrial mobile robots. The proposed architecture allows controlling the KUKA youBot robot remotely through the integration of the Leap Motion device with the Unity 3D graphics engine. The interface allows the operator to control the mobile manipulator by means of pre-established hand movements. A similar problem, but with different focus was addressed by [Brüggemann, Röhling, and Welle \(2015\)](#). The authors proposed an intuitive wearable user interface to control a mobile manipulator, during bomb squads and relief units operations. With the help of IMUs, the movement of the operator arm is recorded and transferred to the manipulator. The operator motion is captured using five IMUs which are integrated into a jacket. The operator arm kinematics is mapped into the manipulator arm kinematics to find the corresponding joint angles. The authors performed standardised tests to evaluate the interface.

Future missions to extraterrestrial destinations raise a high demand for robots that support the astronauts with setting up and maintaining infrastructure on planetary surfaces before and after the crew missions. These robots would be provided with autonomous capabilities since direct teleoperation from Earth would become unpractical due to the increasing communication time delays. Schmaus et al. (2019) proposed a knowledge driven approach for effective teleoperation of a service robot from an orbiting spacecraft. The authors introduced a Human–Robot Interaction (HRI) concept that utilises the autonomous capabilities of the robot to provide the operator with an intuitive interface. Here, the robot perceives the dynamic environment and creates a world representation, on whose basis, only the context-related robot actions are made available to the astronaut. The interface provides the astronaut with the live video of the robot on a tablet. This video is augmented with CAD renderings of the robot world representation to increase the operator awareness. The authors demonstrated with field experiments the viability of the proposed knowledge driven HRI for commanding remote semi-autonomous surface robots.

The teleoperation control of Centauro involves many aspects. Klant et al. (2020) used a simulation-based approach to generate visual feedback which is displayed in a head-mounted device or on arbitrary regular monitors. Based on a digital twin of the real system, 3D simulations are used to visualise the current state of the robot in its environment and to provide semantic information. For locomotion control, a joystick and a pedal controller are provided to the operator, which can also control the leg movements. For manipulation control, a cable-driven 4-DoF arm exoskeleton, a 3-DoF wrist exoskeleton, and an under-actuated hand exoskeleton are used for acquiring the operator arm motion and for transferring back the force and torque feedback.

Almagro et al. (2020) presented an innovative interface that allows a single operator to control multiple agents simultaneously. The proposed solution uses behavioural control scripts, which are programmed during the task preparation and customised or adapted during the execution time. Such scripts allow also the creation of additional behaviours that interconnect multiple agents during the operations. The control scripts are executed on the human–robot interface, which communicates with all the available agents. The authors presented an overall description of the user interface, and outlined all the submodules that enable control of the team of robots in a human-supervisory manner.

In field robotics, the HRI is affected by the communication link between the robot and the human operator such as the network bandwidth, delays, volatility, and security. Human-centred factors such as cognitive limits, psychology and ergonomics play a significant role as well. Szczurek, Prades, Matheson, Rodriguez-Nogueira, and Di Castro (2023) designed, and deployed in the operational scenarios at CERN, a novel MR human–robot interface which exploits augmented-reality and a head-mounted device. The interface interacts with the operator by senses, speech and bare hands, as well as by physical controllers such as a joystick and a keyboard. The interface has different connection options and provided a combination of 2D and 3D contents to the operator head-mounted device. For collaboration between multiple operators, a multi-user architecture is designed, deployed, and tested. This architecture preserves all the control functionalities available to the operator for controlling a single robot. In addition, the architecture allows other operators to connect to the deployed robot, to verify the robot status and feedback and to take control of it.

6. Other types of manipulators

This section discusses documents related to manipulators other than discrete-joint, continuum, and mobile ones. Since the manipulators proposed by those documents belong to a heterogeneous group (non-redundant, redundant, made of soft or rigid mechanisms), they are grouped by topic of interest. Sections 6.1 and 6.2 summarise the modelling and control techniques employed on these manipulators, respectively.

6.1. Modelling

In the context of nuclear fusion, ITER (initially the International Thermonuclear Experimental Reactor) is one of the most ambitious energy projects in the world today. Activation and contamination of structures submitted to high neutron fluxes or in contact with will prevent hands-on maintenance within such structures a few years after beginning operations. Robotic and Remote Handling (RH) systems are considered in ITER as the standard maintenance tools and have been taken into account since the beginning of designing the facility. Access ports or workspaces around each part of the facility needing maintenance will be very limited and significantly impact the size of the maintenance tools. Handling heavy loads in a space-constrained environment is therefore identified as a critical issue for maintenance. Consequently, much effort is spent designing long-reach robotic systems operating in constrained spaces with heavy load manipulation. Furthermore, RH systems are required for various tasks where successful fulfilment depends on system positioning accuracy. However, control of such systems to maintain accurate positioning raises serious difficulties due to their structural and joint flexibility. In these circumstances, Gagarina-Sasia, David, Dubus, Gabellini, Nozais, Perrot, Pretot, Riwan, and Zanardo (2008) performed theoretical and experimental investigations for RH dynamical modelling of systems with significant mechanical flexibility. They proposed using specific mechanical software to replace the cost-bearing experiments with real systems with adequate software models for tuning the corresponding control schemes. They compared software simulations, based on the proposed approach, to the results of natural experiments on a corresponding laboratory mechanical system and to a theoretical linear model. A single-link flexible manipulator with a lumped heavy load was modelled to illustrate the inertia and joint flexibility effects for the long-reach manipulators. Ultimately, this study emphasised that the elasticity effects of the hinge joint are significant in the structure's response.

In the hydropower industry, in situ maintenance work of turbine runners regarding issues such as cavitation damage and cracking is mainly performed manually. Alternatively, the entire turbine requires disassembly and is repaired off-site at a more significant cost. Hazel, Côté, Laroche, and Mongenot (2012) developed an ad hoc robotic technology designed to perform work in situ on hydroelectric equipment. Super COMPact robot Ireq (SCOMPI) is a small, portable, multiprocess manipulator with six DoF. The SCOMPI manipulator comprises links, joints, and drive components, each of which is compliant. Thus, the SCOMPI manipulator behaviour is nonrigid and more complex dynamically than predicted by rigid-body dynamic equations. This work validated a dynamic model by comparing 3D coordinates of the robot's end-effector measured from static experiments and simulation, leading to the result that joint compliance accounts for about 85 % of manipulator flexibility.

Compared with existing kinematics methods, the Product-Of-Exponentials (POE) formula is regarded as one of the most efficient kinematics analysis methods. Unlike the complex coordinate system establishment of each link by the DH method, when applying the POE formula to serial robot kinematics analysis, just the initial twists of joints, spatial frame, and tool frame should be considered. The above characteristics make kinematics modelling based on the POE formula intuitive and efficient. In the surgical sector, tendon-driven configurations are preferred due to their inherent advantages, such as long-distance transmission through limited space, backlash-free under pre-stress of cable, and multiple DoF transmission capability. Unfortunately, the tendon-driven configuration introduces a multi-DoF coupling that further increases the complexity of kinematics analysis of the whole robot, preventing the direct application of the POE formula. He, Wang, Xing, and Wang (2013) proposed a new, effective, and straightforward method to solve this problem. A generic coupled tendon-driven robot is transformed into a pure serial robot by replacing

the robot's DoF coupled with a set of added axes to reestablish a pure serial part that conserves the original local coupling part's functionality. In this way, the POE formula is extended to kinematics analysis and acceleration analysis of coupled tendon-driven robots. In addition, detailed acceleration formulas for serial and coupled tendon-driven robots can also be derived. Finally, this work provides a simulation task and an experiment to validate the kinematics solution and rigour of the presented method.

The DEMONstration Power Plant (DEMO) will be ITER's successor. Inside the DEMO machine, heavy-duty manipulators are foreseen to be widely employed. Experience with heavy-duty robotic machines shows that deformation of the manipulator joints contributes significantly to the end-effector displacement. In order to compensate for such end-effector deformation displacement in the control system in real-time during RH processes of DEMO, it is necessary to develop a computation-effective deformation model of the flexible joints, which can then be integrated and form a deformation model of the whole manipulator. To efficiently compute the deformation of a complex joint, which consists of subjoints, the overall joint deformation model can be derived in the kinematics form of subjoints' deformation by using the matrix structural analysis method, whereas the subjoints are taken as the elementary nodes by applying the same principle as in the FEA but in a larger scale. Li et al. (2018) proposed three modelling methods to construct accurate nodal deformations of the joint: a parametric model, a deterministic ANN model, and a Bayesian ANN model. They considered a specific subjoint from a joint of a boom that is equipped in the Telescopic Articulated Remote Mast (TARM), which operates in the RH and robotics test facility operated by the UK Atomic Energy Authority, as the study object for applying the proposed deformation modelling methods. This study concluded that the parametric model applying the structural mechanics is incompetent in modelling nodal deformation when the nonlinearity in deformation is present. At the same time, both the deterministic ANN and Bayesian ANN managed to model the underlying deformation physics successfully in the subjoint structure, given the amount of training data. In the specific example provided by this document, the performance in both the deterministic ANN model and Bayesian ANN model are equivalent when the same network size is used.

6.2. Control

As stated in Section 6.1, the environment inside ITER torus will be expected to be hostile and dangerous. Due to the expected high level of radiation, all the nominal maintenance in the divertor region of ITER will be carried out with the help of robotic systems. Since the early 2000s, hydraulic manipulators have been considered a good candidate for fusion reactors maintenance. The main advantages of hydraulic manipulators are their large payload to volume and mass, and their reliability and robustness. However, due to their force control limitations, they are disqualified for precise manipulation and are dangerous for the environment and themselves in case of unexpected collision. At that time, the MAESTRO hydraulic manipulator, a radiation-tolerant 120 kg titanium arm with six DoF, was considered the best choice, while requiring conversion to water-hydraulic technology. As described by Measson, David, Louveau, and Friconneau (2003), a prototype of servo-valve that fitted the performances and space constraints of the MAESTRO arm was designed and manufactured. To avoid the mentioned problems, a pressure control servo-valve instead of a flow control servo-valve (standard configuration of the MAESTRO manipulator) was used, leading to a real simplification of the control loop. Indeed, no more pressure sensors were needed to monitor the hydraulic joint in force control mode, and the control law, made of a single loop, was a simple PD controller to control the joint torque from the desired position and speed, plus friction and gravity compensation. In addition, using this kind of valve made significant safety improvements. In fact, in case of electrical failure of the pressure servo-valve, no pressure is

provided to the joints. Then, exploiting mechanical valves, the arm can fall down slowly with a minimum impact on the surrounding environment. As described by Dubus et al. (2008), characterisation tests for specific use in controller-responder mode for teleoperation tasks were conducted in a subsequent phase of the research program. During RH operations, the indirect vision of the operating scene introduces difficulties that can lead to low accuracy performance. Thus, proper force feedback giving the operator an extra sense of touch during manipulation is crucial. For the application described in this work, force feedback was provided to the operator employing a hybrid force-position control scheme. High-quality force control can only be achieved with an excellent real-time compensation of all imperfections of the manipulator mechanical joints, of the arm inertia, and of the gravity (own weight, payload, tool). Reversibility tests provided a good representation of force control loop quality when all compensation models were active, showing that force and position performance of the joint equipped with a water hydraulic servo valve were globally similar or better than that of equipped with an oil servo valve. In parallel, Muhammad et al. (2007) developed a teleoperation system to accomplish a variety of RH operations inside the ITER divertor. Such a system comprises a water hydraulic manipulator as the responder, a commercial haptic device as the controller, a human-machine interface to assist the operator, a vision system comprising cameras and video monitors, and a graphical system providing a virtual 3D view of the environment. The Water Hydraulic MANipulator (WHMAN) was developed as the responder manipulator. The arm of WHMAN is composed of three revolute and one linear joint. A spherical wrist is attached at the end of the arm resulting in improved dexterity and reachability. The Phantom[®] Premium 3.0 6-DoF, providing force feedback in three translational DoF and torque feedback in three rotational DoF, was used as the controller manipulator. The kinematic similarity between Phantom[®] Premium and WHMAN results in the ease of control for the operator. More recently, exploiting the experience of the previous works, Niu, Aha, Mattila, Gotchev, and Ruiz (2019) developed and evaluated a novel software system, 3D Node, which locates and detects the position and orientation of a piece of RH equipment or reactor element to a stereo camera pair. The 3D Node receives images from the stereoscopic cameras and the pose of a manipulator robot's Tool Centre Point from the manipulator control system itself. Additionally, it can receive operator input and provide visual feedback to the operator through its graphical user interface. In summary, the detection information is utilised to adjust the motion trajectories of a robotic manipulator arm.

For decades, anthropomorphic robotic arms with five to seven DoF have been employed in the industry sector. These systems are used for cutting operations on materials, joining materials by welding, material handling in remote and dangerous environments, packing food, inspecting and testing electronic parts and medical products, and several other applications. To accomplish such tasks, the robot arm realises the handling motion on a special trajectory. The robot dynamics might change depending on position and load when used in any industrial application. Applying a controller to this robot manipulator, possible disturbances can be compensated. Haklidir and Tasdelen (2009) modelled and simulated using the commercial modelling and simulation environment Dymola the first three links of a Mitsubishi RV-2AJ Industrial Robot, a 5 axis commercial manipulator, and designed a fuzzy logic controller for the joint angles for the motion trajectory. For this purpose, kinematic equations were obtained and a mathematical model of this system was formed by using Lagrange's Equations.

Robotic manipulators are widely employed in industrial production, especially in hostile, dirty, and dangerous environments. In recent years, there have been more and more needs for surface contact works, such as polishing, grinding, painting, and inspection with robot manipulators. Huang and Enomoto (2009) proposed a hybrid position, posture, force, and moment control as a new concept for a manipulator's contact work to expand the conventional hybrid position and

force control by separating the posture physical vector and the moment physical vector from the position vector and the force vector. Subsequently, to achieve high-speed and high-precision surface contact work by a manipulator, Yao, Huang, Peng, and Oiwa (2011) proposed a separation method of posture components to solve the problem of the rotation order in posture control in hybrid position, posture, force, and moment control. In addition, they proposed introducing impedance characteristics to hybrid position, posture, force and moment control to eliminate the interference between free space and constrained space. Finally, they performed a dynamic simulation of character-erasing motion on the whiteboard of a 6-DoF manipulator.

As mentioned in Section 6.1, in the context of the hydropower industry, Hazel et al. (2012) developed SCOMPI: a new portable manipulator designed with unique track-based kinematics and well suited to accessing turbine blades in a confined space. SCOMPI consists of one prismatic joint for the track and five revolute joints, moved by stepper motors controlled in position. A Position-Velocity-Time motion control strategy is employed to obtain smooth displacement of the end-effector. Since some of the processes performed by the robot, such as grinding and peening, require controlled interaction of the robot with a stiff environment, SCOMPI uses an implicit hybrid force position controller to regulate the grinding power and maintain the desired material removal rate. Thus, the robot is controlled in position and velocity, while the grinding power is adjusted by controlling the robot's position along the surface's normal direction. A curvilinear transform is exploited to decouple the force and position vectors in the Cartesian space. Tool paths are generated in two parametric coordinates tangent to the surface and are controlled in position and velocity, while the parametric coordinate normal to the surface is controlled in force. Robot compliance along this direction is updated continuously as the robot configuration varies. Finally, a feed-forward compensator, which utilises the compliance model of the robot, mentioned in Section 6.1, is implemented to increase the response time without compromising stability.

Over the past decades, robot systems have seen significant technological development, bringing them to unprecedented levels of speed and accuracy and making them invaluable for tasks requiring precise and repetitive motions. These systems can be programmed to work autonomously or guided by human operators when an autonomous operation is infeasible or undesired. In teleoperation frameworks, a remote user can have partial or full access to the robot that accomplishes their goal. With human support, robot systems can perform complex tasks that would be unfeasible to execute autonomously. One of the critical teleoperation applications is task execution exploiting human skill and expertise in remote or extreme environments. In this context, Dwivedi, Gorjup, Kwon, and Liarokapis (2019) presented an intuitive telemanipulation framework for controlling a dexterous robot arm-hand system based on ElectroMyography (EMG) and fiducial marker-based pose tracking. The separate system components were validated, and the complete framework was successfully tested in a remote manipulation setting. The framework proposed in this work is divided into two main groups. The Grasp Identification group focuses on decoding the user's intent and interpreting it for the intuitive control of the New Dexterity adaptive, human-like robot hand. The Arm Trajectory Generation block maps the user's motion to a commercial Universal Robots UR5 robot arm motion. The video stream captured by a head-mounted camera is passed to an image processing module that extracts the fiducial marker pose with respect to the camera frame. The obtained marker pose is passed to the Pose Mapping and Inverse Kinematics module, which maps it to the robot end-effector and computes the corresponding inverse kinematics, obtaining the target robot joint angles. Finally, a closed-loop velocity controller is implemented. Regarding the EMG-based intent decoding, the classification models were trained offline on the acquired data. For each gesture, five trials were recorded with 20 repetitions each. The myoelectric activations of eight muscle groups of the hand and forearm are recorded using

double-differential electrodes. Three different classification algorithms are used to discriminate between the examined gestures based on the acquired EMG data: a Linear Discriminant Analysis (LDA) classifier, a Random Forest (RF) classifier (an ensemble classifier based on decision trees), and a Support Vector Machine (SVM) classifier. The real-time pose-tracking component of the telemanipulation framework is based on the ArUco class of fiducial markers. A reference marker is attached to the user's shoulder to compensate for the subject head motion and consequent shifting of the view angle. The performance of the proposed framework was validated through three sets of experiments. The first set focused on evaluating the ability of the proposed learning algorithm to discriminate between different grasps during offline training, as well as online testing on the robot hand. The second set evaluated the ArUco marker-based pose tracking and mapping system for guiding the robot arm. The last set validated the complete, integrated telemanipulation system in a real-time pick-and-place task. Later on, Shieff, Turner, Dwivedi, Gorjup, and Liarokapis (2021) presented an EMG-based framework that enables the user to take control of the robot platform and perform complex tasks whenever autonomous execution is infeasible. The framework utilises a finite state machine to switch between autonomous and manual EMG-based task execution to control the robot arms and EMG-based gesture identification to control the robot hands without requiring room preparation. The efficiency and intuitiveness of the proposed shared control framework were experimentally validated using a series of grasping experiments.

With humans' continuous development and utilisation of space resources, space robots are gradually becoming essential tools for space activities. This development is essential for increasing human ability to conduct the comprehensive exploration, development, and utilisation of space. A space robot can assist or replace humans in accomplishing specific heavy and dangerous tasks in outer space, such as carrying, assembly, repair, and production. Therefore, researchers from different countries emphasise space robots' dynamics modelling and trajectory tracking control. In this context, the light slim bar represents the best choice for the link of a space manipulator considering launch technologies and the need to reduce launch mass and cost. Compared with a rigid space manipulator, the flexible space manipulator system has many advantages, such as large operation space, low energy consumption, high load mass ratio, and compact component design. To avoid the influences of model uncertainty and suppress the vibration of a flexible manipulator and realise high-accuracy trajectory tracking, Dengfeng and Xiaoqin (2021) constructed a dynamics model of the flexible space manipulator system with an attitude-controlled base. On this basis, they applied a neural network control scheme based on a hybrid trajectory to study the system's rigid motion and flexible vibration suppression. Without loss of generality, assuming a free-floating flexible space manipulator system made of a free-floating base, a rigid link, and a flexible link, this study demonstrated that the proposed control scheme could help the base's attitude and two joints' angles of the space manipulator to track the given desired trajectories effectively and also eliminate vibration of flexible links.

Concerning dangerous high-altitude power grid maintenance operations, Wei, Su, and Guan (2021) proposed a portable and modular controller-responder teleoperation control robot system that combines teleoperation and autonomous motion based on vision and force sensors to perform screw nut operations. In this system, the controller-responder robots are self-designed 5-DoF modular manipulators with the same configuration. First, the responder robot arm performs motion control in the global environment through controller-responder remote operation. Once the robot arm reaches the ideal position, it performs local autonomous fine operations through visual processing and force feedback. Regarding the vision system, when the robot needs to screw the nut autonomously, the identification of the nut's centre position is first performed. Then, according to the relationship between the nut's centre coordinates and the robot base mark, the manipulator can obtain the corresponding position information under the base mark system,

solve the rotation angle of each joint through the inverse kinematics of the robot, and then complete the centring operation of the electric wrench to the centre of the nut through the autonomous movement. Regarding the control system, a hybrid control strategy of force and position is used to operate the nut assembly sleeve. In the entire control framework of mixed force and position, the position information mainly controls the displacement of the end effector in the direction normal to the nut's plane, while the force information adjusts the position of the end effector on the nut's plane. Ultimately, teleoperation frees workers from the dangerous working environment in the entire operation process. At the same time, the robot's autonomous operation based on vision and force improves the accuracy and efficiency of the operation.

The construction industry is one of the most labour-intensive industries in the world. Robotics and automated systems, now highly valued in the construction sector, can potentially revolutionise the industry. In past years, robotic manipulators' reliability, reachability, and precision have significantly improved due to advanced programmability and motion control algorithms, allowing them to efficiently complete monotonous and unsafe tasks. Among the commonly utilised algorithms is the LbCS, which has been successfully utilised for controlled navigation of long-reaching anchored and unanchored robotic arm manipulators. In this context, [Chand, Chand, Narayan, and Naicker \(2022\)](#) presented the derivation of kinematic equations of a new linear robotic system comprising an n -link prismatic arm on an automated slider that undergoes horizontal motion along a rail mounted on a fixed solid base at both ends. Then, they implemented a LbCS to derive the acceleration-based controllers for the mobile slider and its n -link prismatic arm. Finally, they demonstrated the effectiveness of the motion controllers showing that, while moving linearly along the horizontally placed rail, the mobile slider facilitates reachability by placing the end-effector and allowing access to an arbitrary target to accomplish assigned tasks.

Various works are focused on teleoperating robotic systems able to help workers in dangerous environments while performing relatively complex inspection and maintenance tasks. In this context, dual arm robots represent a commonly employed robot category. Examples are given since the early 2000s, like the work provided by [Aracil, Ferre, Hernando, Pinto, and Sebastian \(2002\)](#). In this work, a teleoperation system called ROBTET performs complex tasks such as changing insulator sets, opening and closing switches, and inspecting or changing line equipment in the context of maintaining electrical live-power lines. The ROBTET system works in a semi-automatic control mode, with the operator sending commands from the cabin on the truck and receiving information from the remote working environment. Dual arm manipulators based on a hydraulic system are teleoperated by a human operator sitting in a vehicle required to place the telerobotic system over the desired line. Telemanipulators and tools are placed on a remote platform located on an isolated telescopic boom. The system control is based on a controller-responder approach that pays great attention to providing complete visual, tactile, and force feedback to the operator while allowing the robot to autonomously avoid collisions or touching the high-voltage components of the live-power line. In a similar application, also focused on inspecting and maintaining power lines with dual arm robots, [Li et al. \(2016\)](#) proposed a reliable tracking algorithm for hot-line dual arm robots. This work aimed to guarantee the security, precision, and dynamic property of the hot-line dual-arm operations employing a controller-responder tracking control method, using Dynamic Matrix Control (DMC) software for modelling and simulation. The simulations show that the DMC theory can successfully be applied to achieve precise control of the hot-line dual arm robots. In the framework of dual arm operation, [Liu, Lei, Han, Xu, and Zou \(2016\)](#) provided insight into motion planning and control for dual arm coordination. This work presents three types of resolved motion control methods for a humanoid robot during coordinated manipulation: position-level, velocity-level, and acceleration-level resolved motion control methods. The desired pose, velocity, and acceleration of each end-effector are resolved according to the desired motion of the payload

and the constraints on the closed-chain system without consideration of the internal force. For each case, the joint variables of each arm are then calculated using the inverse kinematic equations at position-level, velocity-level, or acceleration-level. Then, a dynamic modelling and simulation platform is developed and the proposed methods are verified by typical cases. Finally, dual arm robots play an essential role in space applications as well. A famous example is given by the Special Purpose Dexterous Manipulator (SPDM) known as Dextre, a specific component of the Canada's Mobile Servicing System (MSS). Dextre's primary role on the International Space Station (ISS), with a particular focus on how these will help optimise the use of crew resources on the ISS, is discussed by [Coleshill et al. \(2009\)](#). [Li et al. \(2010\)](#) presented a dual arm space robot design method, including the mechanism, integrative joint, vision system, and vision-based climbing trajectory plan, as well as the joints' control performance. By exploiting the vision-based climbing trajectory plane, the designed dual arm space robot system can climb about in the horizontal plane. Since the vision system introduces errors, a force control for the robot hand is implemented.

7. Conclusion

The use of robotic systems for inspection and maintenance is gaining importance since they can operate in challenging environments that are hazardous or inaccessible to humans. A preliminary investigation revealed that manipulators represent a significant proportion of the robotic systems employed in this context. Hence, this article aims to provide a systematic literature review about modelling and controlling manipulators for inspection and maintenance tasks in challenging environments. Among these robotic systems, the most widespread are hyper-redundant discrete-joint manipulators, continuum manipulators, and mobile manipulators. Over the years, the nuclear-related industry has been the leading driver for the research on manipulators designed for challenging environments. In parallel, several manipulators have been developed to accomplish general-purpose inspection and maintenance tasks or operate in confined and constrained environments.

The systematic literature review discloses that discrete-joint hyper-redundant manipulators are applied almost with the same frequency in nuclear-related industries, confined and constrained environments, and general-purpose inspection and maintenance tasks. In general, most documents are about design, modelling and control concurrently. Specifically, about half is about designing or modelling techniques for discrete-joint hyper-redundant manipulators. Instead, the documents dealing with control algorithms implemented on this type of robot attain two-thirds of the total. Through the years, the research has mainly focused on exploiting the benefit of hyper-redundancy, investigating kinematic models to obtain increasingly efficient kinematic control algorithms to implement in real-time. Several works also proposed machine learning methods to model and compensate for static deformation to improve positioning accuracy. These studies have reached such maturity that they can be applied to real scenarios. On the contrary, although some works deal with dynamic models and dynamic control algorithms to further improve trajectory tracking and obtain better dynamic performance, these algorithms are difficult to implement in real applications due to the high computational effort required to deal with the high number of degrees of freedom and due to the complex identification procedures of dynamic parameters like friction and inertias. For this reason, dynamic modelling and control of discrete-joint hyper-redundant manipulators is still a fertile field of research.

The systematic literature review illustrates that continuum manipulators are mainly employed in the aviation industry, for inspecting and maintaining aero-engines and fuel tanks, and in medicine, especially for surgery and endoscopy. Mechanical compliance and intrinsic kinematic redundancy are the most important features of continuum manipulators working in fragile environments like aero-engines or human bodies. For this reason, the works retrieved in this literature review highlight

that the main topics faced by researchers studying this kind of robot are the mechanical design, the kinematic model, and the kinematic control. Conversely, as for discrete-joint hyper-redundant manipulators, the dynamic modelling and control of continuum manipulators are not equally investigated. As hyper-redundant (often cable-driven) manipulators, the dynamic modelling of continuum manipulators is affected by many of the difficulties described above for discrete-joint manipulators. However, the leading causes of this scarcity of focus on robot dynamics are likely the under-actuation characterising continuum robots and the complexity of modelling the dynamics of a continuum body, which is frequently further complicated by flexibility.

The systematic literature review indicates that mobile manipulators are mainly developed to accomplish general-purpose inspection and maintenance tasks in terrestrial, aerial, and underwater environments. Regarding the operating sector, the nuclear-related industry is the most common. The main topics covered by the documents that describe such mobile manipulators are control, teleoperation, design, and modelling. Throughout the years, significant effort has been made in designing, modelling, and controlling this type of robot. Indeed, mobile manipulators present a broad set of challenges. These systems require sensors and sensor fusion algorithms for localisation and navigation. Control laws and path-planning algorithms are necessary to effectively move the mobile platform toward the desired position. Furthermore, the manipulators require specific control laws to perform the desired actions. At the same time, defining kinematic and dynamic models of a mobile manipulator is challenging because the floating base degrees of freedom are combined with the ones of the robotic arm. Finally, teleoperation interfaces are usually developed to facilitate single or multiple operators' remote control over these mobile manipulators. Given that, designing effective control strategies and intuitive teleoperation interfaces for accomplishing demanding inspection missions represent some of the open challenges in the context of inspection and maintenance applications in challenging environments operated by mobile manipulators.

Finally, the systematic literature review shows many documents belonging to a heterogeneous group of robots comprising non-redundant and redundant manipulators made of soft or rigid mechanisms. The primary application environments for these robots are the nuclear, energy, space, and industry sectors. A significant proportion of the documents describing such robots focus on modelling, control, and teleoperation.

Ultimately, the results of this systematic literature review indicate that modelling and controlling manipulators designed for inspection and maintenance activities in challenging environments is a fertile research field.

Declaration of competing interest

The authors declare that they have no known competing financial interests or personal relationships that could have appeared to influence the work reported in this paper.

Data availability

No data was used for the research described in the article.

References

- Amouri, A., Cherfia, A., Belkhir, A., & Merabti, H. (2023). Bio-inspired a novel dual-cross-module sections cable-driven continuum robot: design, kinematics modeling and workspace analysis. *Journal of the Brazilian Society of Mechanical Sciences and Engineering*, 45(5), 265.
- Aracil, R., Ferre, M., Hernando, M., Pinto, E., & Sebastian, J. (2002). Telerobotic system for live-power line maintenance: ROBTET. *Control Engineering Practice*, 10(11), 1271–1281. [http://dx.doi.org/10.1016/S0967-0661\(02\)00182-X](http://dx.doi.org/10.1016/S0967-0661(02)00182-X).
- Aristidou, A., & Lasenby, J. (2011). FABRIK: A fast, iterative solver for the inverse kinematics problem. *Graphical Models*, 73(5), 243–260.
- Ba, W., Dong, X., Mohammad, A., Wang, M., Axinte, D., & Norton, A. (2021). Design and validation of a novel fuzzy-logic-based static feedback controller for tendon-driven continuum robots. *IEEE/ASME Transactions on Mechatronics*, 26(6), 3010–3021.
- Ben-Gharbia, K. M., Maciejewski, A. A., & Roberts, R. G. (2013). Kinematic design of redundant robotic manipulators for spatial positioning that are optimally fault tolerant. *IEEE Transactions on Robotics*, 29(5), 1300–1307.
- Bláha, L., & Svejda, M. (2018). Path planning of hyper-redundant manipulator in developed view. In *2018 19th international carpathian control conference* (pp. 295–300). IEEE.
- Brüggemann, B., Röhling, T., & Welle, J. (2015). Coupled human-machine tele-manipulation. *Procedia Manufacturing*, 3, 998–1005.
- Buckingham, R., & Graham, A. (2012). Nuclear snake-arm robots. *Industrial Robot: An International Journal*.
- Campisano, F., Ramirez, A. A., Caló, S., Chandler, J. H., Obstein, K. L., Webster, R. J., et al. (2020). Online disturbance estimation for improving kinematic accuracy in continuum manipulators. *IEEE Robotics and Automation Letters*, 5(2), 2642–2649.
- Campisano, F., Ramirez, A. A., Landewee, C. A., Caló, S., Obstein, K. L., Webster, R. J., et al. (2020). Teleoperation and contact detection of a waterjet-actuated soft continuum manipulator for low-cost gastroscopy. *IEEE Robotics and Automation Letters*, 5(4), 6427–6434.
- Canali, C., Pistone, A., Ludovico, D., Guardiani, P., Gagliardi, R., De Mari Casareto Dal Verme, L., et al. (2022). Design of a novel long-reach cable-driven hyper-redundant snake-like manipulator for inspection and maintenance. *Applied Sciences*, 12(7), 3348.
- Chalfoun, J., Bidard, C., Keller, D., Perrot, Y., & Piolain, G. (2007). Design and flexible modeling of a long reach articulated carrier for inspection. In *2007 IEEE/RSJ international conference on intelligent robots and systems* (pp. 4013–4019). IEEE.
- Chand, R., Chand, R. P., Narayan, S. V., & Naicker, P. R. (2022). Autonomous linear slider with extendable robotic arm for increased reachability. In *2022 IEEE Asia-Pacific conference on computer science and data engineering* (pp. 1–6). IEEE.
- Cobos-Guzman, S., Palmer, D., & Axinte, D. (2017). Kinematic model to control the end-effector of a continuum robot for multi-axis processing. *Robotica*, 35(1), 224–240.
- Cocuzza, S., & Doria, A. (2021). Modeling and identification of vibrations in a UAV for aerial manipulation. In *Advances in Italian mechanism science: proceedings of the 3rd international conference of iToMM Italy 3* (pp. 182–190). Springer.
- Coleshill, E., Oshinowo, L., Rembala, R., Bina, B., Rey, D., & Sindelar, S. (2009). Dextre: Improving maintenance operations on the international space station. *Acta Astronautica*, 64(9), 869–874. <http://dx.doi.org/10.1016/j.actaastro.2008.11.011>, URL: <https://www.sciencedirect.com/science/article/pii/S0094576508003627>.
- Cruz Ulloa, C., Domínguez, D., Del Cerro, J., & Barrientos, A. (2022). A mixed-reality tele-operation method for high-level control of a legged-manipulator robot. *Sensors*, 22(21), 8146.
- De Mari Casareto Dal Verme, L., Ludovico, D., Pistone, A., Canali, C., & Caldwell, D. G. (2023). Lyapunov stability of cable-driven manipulators with synthetic fibre cables regulated by non-linear full-state feedback controller. *ISA Transactions*, 142, 360–371.
- Delgado López-Cózar, E., Orduña-Malea, E., & Martín-Martín, A. (2019). Google scholar as a data source for research assessment. In *Springer handbook of science and technology indicators* (pp. 95–127). Springer.
- Dengfeng, H., & Xiaoqin, H. (2021). Neural network compensation control for model uncertainty of flexible space manipulator based on hybrid trajectory. *Journal of Engineering Science & Technology Review*, 14(1).
- Dong, X., Axinte, D., Palmer, D., Cobos, S., Raffles, M., Rabani, A., et al. (2017). Development of a slender continuum robotic system for on-wing inspection/repair of gas turbine engines. *Robotics and Computer-Integrated Manufacturing*, 44, 218–229.
- Dong, X., Palmer, D., Axinte, D., & Kell, J. (2019). In-situ repair/maintenance with a continuum robotic machine tool in confined space. *Journal of Manufacturing Processes*, 38, 313–318.
- Dubus, G., David, O., Nozais, F., Measson, Y., Friconeau, J. P., & Palmer, J. (2008). Assessment of a water hydraulic joint for remote handling operations in the divertor region. *Fusion Engineering and Design*, 83(10–12), 1845–1849.
- Dwivedi, A., Gorjup, G., Kwon, Y., & Liarokapis, M. (2019). Combining electromyography and fiducial marker based tracking for intuitive telemanipulation with a robot arm hand system. In *2019 28th IEEE international conference on robot and human interactive communication* (pp. 1–6). IEEE.
- Endo, G., Horigome, A., & Takata, A. (2019). Super dragon: A 10-m-long-coupled tendon-driven articulated manipulator. *IEEE Robotics and Automation Letters*, 4(2), 934–941.
- English, J. D., & Maciejewski, A. A. (1998). Fault tolerance for kinematically redundant manipulators: Anticipating free-swinging joint failures. *IEEE Transactions on Robotics and Automation*, 14(4), 566–575.
- Fang, Y., Dong, X., Mohammad, A., & Axinte, D. (2023). Design and control of a multiple-section continuum robot with a hybrid sensing system. *IEEE/ASME Transactions on Mechatronics*.
- Gagarina-Sasia, T., David, O., Dubus, G., Gabellini, E., Nozais, F., Perrot, Y., et al. (2008). Remote handling dynamical modelling: Assessment of a new approach to enhance positioning accuracy with heavy load manipulation. *Fusion Engineering and Design*, 83(10–12), 1856–1860.

- Garcia, C. A., Naranjo, J. E., Campana, L. A., Castro, M., Beltran, C., & Garcia, M. V. (2018). Flexible robotic teleoperation architecture under IEC 61499 standard for oil & gas process. 1, In *2018 IEEE 23rd international conference on emerging technologies and factory automation* (pp. 1269–1272). IEEE.
- Giustini, D., & Boulos, M. N. K. (2013). Google scholar is not enough to be used alone for systematic reviews. *Online Journal of Public Health Informatics*, 5(2), 214.
- Gong, Z., Chen, B., Liu, J., Fang, X., Liu, Z., Wang, T., et al. (2019). An opposite-bending-and-extension soft robotic manipulator for delicate grasping in shallow water. *Frontiers in Robotics and AI*, 6, 26.
- Gong, Z., Fang, X., Chen, X., Cheng, J., Xie, Z., Liu, J., et al. (2021). A soft manipulator for efficient delicate grasping in shallow water: Modeling, control, and real-world experiments. *International Journal of Robotics Research*, 40(1), 449–469.
- Guardiani, P., Ludovico, D., Pistone, A., Abidi, H., Zaplana, I., Lee, J., et al. (2022). Design and analysis of a fully actuated cable-driven joint for hyper-redundant robots with optimal cable routing. *Journal of Mechanisms and Robotics*, 14(2).
- Guochen, N., Li, W., Qingji, G., & Dandan, H. (2014). Path-tracking algorithm for aircraft fuel tank inspection robots. *International Journal of Advanced Robotic Systems*, 11(5), 82.
- Haklidi, M., & Tasdelen, I. (2009). Modeling, simulation and fuzzy control of an anthropomorphic robot arm by using Dymola. *Journal of Intelligent Manufacturing*, 20(2), 177–186.
- Hazel, B., Côté, J., Laroche, Y., & Mongenot, P. (2012). A portable, multiprocess, track-based robot for in situ work on hydropower equipment. *Journal of Field Robotics*, 29(1), 69–101.
- He, C., Wang, S., Xing, Y., & Wang, X. (2013). Kinematics analysis of the coupled tendon-driven robot based on the product-of-exponentials formula. *Mechanism and Machine Theory*, 60, 90–111.
- Hebert, P., Bajracharya, M., Ma, J., Hudson, N., Aydemir, A., Reid, J., et al. (2015). Mobile manipulation and mobility as manipulation—design and algorithms of RoboSimian. *Journal of Field Robotics*, 32(2), 255–274.
- Hilario, J., Penaloza, C., Hernandez-Carmona, D., Balbuena, J., Quiroz, D., Ramirez, J., et al. (2019). Development of a mobile robot for inspection of analog gauges in industrial plants using computer vision. In *2019 IEEE international conference on cybernetics and intelligent systems (CIS) and IEEE conference on robotics, automation and mechatronics (RAM)* (pp. 209–214). IEEE.
- Holmberg, R., & Khatib, O. (2000). Development and control of a holonomic mobile robot for mobile manipulation tasks. *International Journal of Robotics Research*, 19(11), 1066–1074.
- Hong, W., Feng, F., Xie, L., & Yang, G.-Z. (2022). A two-segment continuum robot with piecewise stiffness for maxillary sinus surgery and its decoupling method. *IEEE/ASME Transactions on Mechatronics*, 27(6), 4440–4450.
- Hong, W., Xie, L., Liu, J., Sun, Y., Li, K., & Wang, H. (2018). Development of a novel continuum robotic system for maxillary sinus surgery. *IEEE/ASME Transactions on Mechatronics*, 23(3), 1226–1237.
- Hong, W., Zhou, Y., Cao, Y., Feng, F., Liu, Z., Li, K., et al. (2022). Development and validation of a two-segment continuum robot for maxillary sinus surgery. *The International Journal of Medical Robotics and Computer Assisted Surgery*, 18(1), Article e2340.
- Horigome, A., & Endo, G. (2018). Investigation of repetitive bending durability of synthetic fiber ropes. *IEEE Robotics and Automation Letters*, 3(3), 1779–1786.
- Horigome, A., Yamada, H., Endo, G., Sen, S., Hirose, S., & Fukushima, E. F. (2014). Development of a coupled tendon-driven 3D multi-joint manipulator. In *2014 IEEE international conference on robotics and automation* (pp. 5915–5920). IEEE.
- Huang, Y., Yan, L., Yang, T., Hu, Z., & Xu, W. (2023). Sensing design, trajectory planning, and motion control of a cable-driven redundant manipulator composed of quaternion joints. *Journal of Mechanisms and Robotics*, 15(5), Article 055001.
- Huanga, Q., & Enomoto, R. (2009). Hybrid position, posture, force and moment control of robot manipulators. In *2008 IEEE international conference on robotics and biomimetics* (pp. 1444–1450). IEEE.
- Jamisola, R. S., Maciejewski, A. A., & Roberts, R. G. (2006). Failure-tolerant path planning for kinematically redundant manipulators anticipating locked-joint failures. *IEEE Transactions on Robotics*, 22(4), 603–612.
- Jones, B. A., & Walker, I. D. (2006). Kinematics for multisection continuum robots. *IEEE Transactions on Robotics*, 22(1), 43–55.
- Ju, R., Zhang, D., Xu, J., Yuan, H., Miao, Z., Zhou, M., et al. (2022). Design, modeling, and kinematics analysis of a modular cable-driven manipulator. *Journal of Mechanisms and Robotics*, 14(6), Article 060903.
- Keller, D., Perrot, Y., Gargiulo, L., Friconneau, J. P., Bruno, V., Le, R., et al. (2008). Demonstration of an ITER relevant remote handling equipment for tokamak close inspection. In *2008 IEEE/RSJ international conference on intelligent robots and systems* (pp. 1495–1500). IEEE.
- Khamseh, H. B., Janabi-Sharifi, F., & Abdessameud, A. (2018). Aerial manipulation—A literature survey. *Robotics and Autonomous Systems*, 107, 221–235.
- Kim, S., Jung, S. H., & Kim, C. H. (1999). Preventive maintenance and remote inspection of nuclear power plants using tele-robotics. In *Proceedings 1999 IEEE/RSJ international conference on intelligent robots and systems. human and environment friendly robots with high intelligence and emotional quotients (cat. no. 99CH36289), vol. 1* (pp. 603–608). IEEE.
- Kim, Y. J., Kim, J. I., & Jang, W. (2018). Quaternion joint: Dexterous 3-DOF joint representing quaternion motion for high-speed safe interaction. In *2018 IEEE/RSJ international conference on intelligent robots and systems* (pp. 935–942). IEEE.
- Klamt, T., Schwarz, M., Lenz, C., Baccelliere, L., Buongiorno, D., Cichon, T., et al. (2020). Remote mobile manipulation with the centauRO robot: Full-body telepresence and autonomous operator assistance. *Journal of Field Robotics*, 37(5), 889–919.
- Lewis, C. L., & Maciejewski, A. A. (1997). Fault tolerant operation of kinematically redundant manipulators for locked joint failures. *IEEE Transactions on Robotics and Automation*, 13(4), 622–629.
- Li, A., Fan, M., Song, R., Li, Y., Zhang, S., & Xu, P. (2016). DMC based tracking algorithm for hot-line dual-arm robots. In *2016 IEEE international conference on information and automation* (pp. 25–30). <http://dx.doi.org/10.1109/ICInfA.2016.7831792>.
- Li, H., Huang, Q., Dong, Q., Li, C., He, Y., Jiang, Z., et al. (2010). Design for a dual-arm space robot. In *ROMANSy 18 robot design, dynamics and control: Proceedings of the eighteenth CISM-iFToMM symposium* (pp. 191–198). Springer.
- Li, M., Wu, H., Handroos, H., Skilton, R., Keep, J., & Loving, A. (2018). Comparison of deformation models of flexible manipulator joints for use in DEMO. *IEEE Transactions on Plasma Science*, 46(5), 1198–1204.
- Liu, T., Lei, Y., Han, L., Xu, W., & Zou, H. (2016). Coordinated resolved motion control of dual-arm manipulators with closed chain. *International Journal of Advanced Robotic Systems*, 13(3), 80. <http://dx.doi.org/10.5772/63430>.
- Liu, S., Yang, Z., Zhu, Z., Han, L., Zhu, X., & Xu, K. (2016). Development of a dexterous continuum manipulator for exploration and inspection in confined spaces. *Industrial Robot: An International Journal*, 43(3), 284–295.
- Ludovico, D., Pistone, A., Dal Verme, L. D. M. C., Guardiani, P., Caldwell, D. G., & Canali, C. (2021). Static elasticity compensation via recursive artificial neural network for long-reach cable-driven hyper-redundant manipulators. In *2021 20th international conference on advanced robotics* (pp. 1116–1120). IEEE.
- Luo, Q., Hu, Q., Zhang, Y., & Sun, Y. (2022). Segmented hybrid motion-force control for a hyper-redundant space manipulator. *Aerospace Science and Technology*, 131, Article 107981.
- Ma, S., Hirose, S., & Yoshinada, H. (1994). Development of a hyper-redundant multi-joint manipulator for maintenance of nuclear reactors. *Advanced Robotics*, 9(3), 281–300.
- Mahl, T., Hildebrandt, A., & Sawodny, O. (2014). A variable curvature continuum kinematics for kinematic control of the bionic handling assistant. *IEEE Transactions on Robotics*, 30(4), 935–949.
- Marais, W. J., & Göktogan, A. H. (2017a). Design and control of CRAM: A highly articulated cable-driven remote access manipulator for confined space inspection. In *Proceedings of the Australasian conference on robotics and automation* (pp. 11–13).
- Marais, W., & Göktogan, A. (2017b). A new manipulability measure for the control of CRAM: A cable-driven remote access manipulator. In *Proceedings of the Australasian conference on robotics and automation* (pp. 11–13).
- Martin, A., Barrientos, A., & Del Cerro, J. (2018). The natural-CCD algorithm, a novel method to solve the inverse kinematics of hyper-redundant and soft robots. *Soft Robotics*, 5(3), 242–257.
- Martín-Barrio, A., Roldán-Gómez, J. J., Rodríguez, I., Del Cerro, J., & Barrientos, A. (2020). Design of a hyper-redundant robot and teleoperation using mixed reality for inspection tasks. *Sensors*, 20(8), 2181.
- Martin-Martin, A., Thelwall, M., Orduna-Malea, E., & Delgado López-Cózar, E. (2021). Google Scholar, Microsoft Academic, Scopus, Dimensions, Web of Science, and OpenCitations' COCI: a multidisciplinary comparison of coverage via citations. *Scientometrics*, 126(1), 871–906.
- Mavinkurve, U., Kanada, A., Tafirishi, S. A., Honda, K., Nakashima, Y., & Yamamoto, M. (2023). Geared rod-driven continuum robot with woodpecker-inspired extension mechanism and IMU-based force sensing. *IEEE Robotics and Automation Letters*, 9(1), 135–142.
- Measson, Y., David, O., Louveau, F., & Friconneau, J. (2003). Technology and control for hydraulic manipulators. *Fusion Engineering and Design*, 69(1–4), 129–134.
- Meng, D., Xu, H., Xu, H., Sun, H., & Liang, B. (2023). Trajectory tracking control for a cable-driven space manipulator using time-delay estimation and nonsingular terminal sliding mode. *Control Engineering Practice*, 139, Article 105649.
- Mu, Z., Chen, Y., Li, Z., Qian, H., & Ding, N. (2021). A spatial biarc method for inverse kinematics and configuration planning of concentric cable-driven manipulators. *IEEE Transactions on Systems, Man, and Cybernetics: Systems*, 52(7), 4177–4186.
- Mu, Z., Yuan, H., Xu, W., Hu, Z., Liu, T., & Liang, B. (2019). Simultaneous planning method considering both overall configuration and end pose for hyper-redundant manipulators. *IEEE Access*, 7, 136842–136854.
- Muhammad, A., Esque, S., Mattila, J., Tolonen, M., Nieminen, P., Linna, O., et al. (2007). Development of water hydraulic remote handling system for divertor maintenance of ITER. In *2007 IEEE 22nd symposium on fusion engineering* (pp. 1–4). IEEE.
- Niu, L., Aha, L., Mattila, J., Gotchev, A., & Ruiz, E. (2019). A stereoscopic eye-in-hand vision system for remote handling in ITER. *Fusion Engineering and Design*, 146, 1790–1795.
- Niu, P., Han, L., Huang, Y., & Yan, L. (2024). Shape-controllable inverse kinematics of hyper-redundant robots based on the improved FABRIK method. *Robotica*, 42(1), 225–241.
- Niu, G., Wang, L., & Zong, G. (2015). Attitude control based on fuzzy logic for continuum aircraft fuel tank inspection robot. *Journal of Intelligent & Fuzzy Systems*, 29(6), 2495–2503.

- Ollero, A., Tognon, M., Suarez, A., Lee, D., & Franchi, A. (2021). Past, present, and future of aerial robotic manipulators. *IEEE Transactions on Robotics*, 38(1), 626–645.
- Paljug, E., Ohm, T., & Hayati, S. (1995). The JPL serpentine robot: a 12-DOF system for inspection. In *Proceedings of 1995 IEEE international conference on robotics and automation*, vol. 3 (pp. 3143–3148). IEEE.
- Peng, J., Zhang, C., Ge, D., & Han, Y. (2022). Two trajectory tracking control methods for space hyper-redundant cable-driven robots considering model uncertainty. *Multibody System Dynamics*, 56(2), 123–152.
- Peng, J., Zhang, C., Meng, D., & Liang, B. (2023). Trajectory optimization methods of a space hyper-redundant robot based on effective arm-shape measurement. *IEEE Transactions on Instrumentation and Measurement*.
- Phillips, B. T., Becker, K. P., Kurumaya, S., Galloway, K. C., Whittredge, G., Vogt, D. M., et al. (2018). A dexterous, glove-based teleoperable low-power soft robotic arm for delicate deep-sea biological exploration. *Scientific Reports*, 8(1), 14779.
- Prados Sesmero, C., Buonocore, L. R., & Di Castro, M. (2021). Omnidirectional robotic platform for surveillance of particle accelerator environments with limited space areas. *Applied Sciences*, 11(14), 6631.
- Qi, F., Dou, X., Bai, D., Zhang, H., Pei, H., & Zhu, J. (2023). Kinematics analysis, motion planning and control of the continuum manipulator in minimally invasive surgery. *Proceedings of the Institution of Mechanical Engineers, Part C (Mechanical Engineering Science)*, Article 09544062221148598.
- Qin, G., Wang, Q., Li, C., Ji, A., Wu, H., Yang, Z., et al. (2023). Design and development of a cable-driven elephant trunk robot with variable cross-sections. *Industrial Robot: the International Journal of Robotics Research and Application*, 50(3), 520–529.
- Qin, G., Wu, H., & Ji, A. (2023). Variable-curvature elephant trunk robot in nuclear industry. *Fusion Engineering and Design*, 192, Article 113642.
- Rocha, F., Garcia, G., Pereira, R. F., Faria, H. D., Silva, T. H., Andrade, R. H., et al. (2021). Rosi: A robotic system for harsh outdoor industrial inspection-system design and applications. *Journal of Intelligent and Robotic Systems*, 103, 1–22.
- Ruggiero, F., Lippiello, V., & Ollero, A. (2018). Aerial manipulation: A literature review. *IEEE Robotics and Automation Letters*, 3(3), 1957–1964.
- Schmaus, P., Leidner, D., Krüger, T., Bayer, R., Pleintinger, B., Schiele, A., et al. (2019). Knowledge driven orbit-to-ground teleoperation of a robot coworker. *IEEE Robotics and Automation Letters*, 5(1), 143–150.
- Schwarz, M., Rodehutsors, T., Droschel, D., Beul, M., Schreiber, M., Araslanov, N., et al. (2017). Nimbro rescue: solving disaster-response tasks with the mobile manipulation robot momaro. *Journal of Field Robotics*, 34(2), 400–425.
- Sciavicco, L., & Siciliano, B. (1988). A solution algorithm to the inverse kinematic problem for redundant manipulators. *IEEE Journal of Robotics and Automation*, 4(4), 403–410.
- Selem, I. A., El-Hussieny, H., & Assal, S. F. M. (2018). Motion planning for continuum robots: A learning from demonstration approach. In *2018 27th IEEE international symposium on robot and human interactive communication* (pp. 868–873). IEEE.
- Sharma, B., Singh, S., Vanualailai, J., & Prasad, A. (2018). Globally rigid formation of n-link doubly nonholonomic mobile manipulators. *Robotics and Autonomous Systems*, 105, 69–84.
- She, Y., Xu, W., Su, H., Liang, B., & Shi, H. (2016). Fault-tolerant analysis and control of SSRMS-type manipulators with single-joint failure. *Acta Astronautica*, 120, 270–286.
- Shi, S., Cheng, Y., Pan, H., Zhao, W., & Wu, H. (2018). Development and error compensation of a flexible multi-joint manipulator applied in nuclear fusion environment. In *2018 IEEE/RSJ international conference on intelligent robots and systems* (pp. 3587–3592). IEEE.
- Shieff, D., Turner, A., Dwivedi, A., Gorjup, G., & Liarokapis, M. (2021). An electromyography based shared control framework for intuitive robotic telemanipulation. In *2021 20th international conference on advanced robotics* (pp. 806–811). <http://dx.doi.org/10.1109/ICAR53236.2021.9659463>.
- Siciliano, B., & Khatib, O. (Eds.). (2016). *Springer handbooks, Springer Handbook of Robotics*. Springer, <http://dx.doi.org/10.1007/978-3-319-32552-1>.
- Singh, V. K., Singh, P., Karmakar, M., Leta, J., & Mayr, P. (2021). The journal coverage of web of science, scopus and dimensions: A comparative analysis. *Scientometrics*, 126, 5113–5142.
- Sofla, M. S., Sadigh, M. J., Sadati, S. H., Bergeles, C., & Zareinejad, M. (2023). Sliding-surface dynamic control of a continuum manipulator with large workspace. *Control Engineering Practice*, 141, Article 105680.
- Su, Y., Chen, X., Zhou, T., Pretty, C., & Chase, G. (2022). Mixed reality-integrated 3D/2D vision mapping for intuitive teleoperation of mobile manipulator. *Robotics and Computer-Integrated Manufacturing*, 77, Article 102332.
- Szczurek, K. A., Prades, R. M., Matheson, E., Rodriguez-Nogueira, J., & Di Castro, M. (2023). Multimodal multi-user mixed reality human–robot interface for remote operations in hazardous environments. *IEEE Access*, 11, 17305–17333.
- Taiwei, Y., Huang, J., Wenfu, X., Ke, S., & Liang, B. (2023). Development of a cable-driven redundant space manipulator with large bending angle by combining quaternion joints and segmented coupled linkages mechanism. *Chinese Journal of Aeronautics*, 36(11), 483–499.
- Talas, S. K., Baydere, B. A., Altinsoy, T., Tutcu, C., & Samur, E. (2020). Design and development of a growing pneumatic soft robot. *Soft Robotics*, 7(4), 521–533.
- Tang, J., Zhang, Y., Huang, F., Li, J., Chen, Z., Song, W., et al. (2019). Design and kinematic control of the cable-driven hyper-redundant manipulator for potential underwater applications. *Applied Sciences*, 9(6), 1142.
- Troncoso, D. A., Robles-Linares, J. A., Russo, M., Elbanna, M. A., Wild, S., Dong, X., et al. (2022). A continuum robot for remote applications: From industrial to medical surgery with slender continuum robots. *IEEE Robotics & Automation Magazine*.
- Veiga Almagro, C., Lunghi, G., Di Castro, M., Centelles Beltran, D., Marín Prades, R., Masi, A., et al. (2020). Cooperative and multimodal capabilities enhancement in the CERNTAURO human–robot interface for hazardous and underwater scenarios. *Applied Sciences*, 10(17), 6144.
- Villedieu, E., Bruno, V., Pastor, P., Gargiulo, L., Song, Y., Cheng, Y., et al. (2016). An articulated inspection arm for fusion purposes. *Fusion Engineering and Design*, 109, 1480–1486.
- Wang, M., Dong, X., Ba, W., Mohammad, A., Axinte, D., & Norton, A. (2021). Design, modelling and validation of a novel extra slender continuum robot for in-situ inspection and repair in aeroengine. *Robotics and Computer-Integrated Manufacturing*, 67, Article 102054.
- Wang, J., Hu, C., Ning, G., Ma, L., Zhang, X., & Liao, H. (2023). A novel miniature spring-based continuum manipulator for minimally invasive surgery: Design and evaluation. *IEEE/ASME Transactions on Mechatronics*.
- Wang, M., Palmer, D., Dong, X., Alatorre, D., Axinte, D., & Norton, A. (2018). Design and development of a slender dual-structure continuum robot for in-situ aeroengine repair. In *2018 IEEE/RSJ international conference on intelligent robots and systems* (pp. 5648–5653). IEEE.
- Wang, C., Xie, H., & Yang, H. (2023). An iterative path-following method for hyper-redundant snake-like manipulator with joint limits. *Industrial Robot: The International Journal of Robotics Research and Application*, 50(3), 505–519.
- Wei, H., Su, M., & Guan, Y. (2021). Semi-autonomous robotic manipulation by teleoperation with master-slave robots and autonomy based on vision and force sensing. In *Intelligent robotics and applications: 14th international conference, ICIRA 2021, Yantai, China, October 22–25, 2021, proceedings, part i 14* (pp. 36–46). Springer.
- Wild, S., Zeng, T., Mohammad, A., Billingham, J., Axinte, D., & Dong, X. (2024). Efficient and scalable inverse kinematics for continuum robots. *IEEE Robotics and Automation Letters*.
- Wu, H., Yu, J., Pan, J., Li, G., & Pei, X. (2022). CRRIK: A fast heuristic algorithm for the inverse kinematics of continuum robot. *Journal of Intelligent and Robotic Systems*, 105(3), 55.
- Xie, H., Wang, C., Li, S., Hu, L., & Yang, H. (2019). A geometric approach for follow-the-leader motion of serpentine manipulator. *International Journal of Advanced Robotic Systems*, 16(5), Article 1729881419874638.
- Xu, S., & He, B. (2022). Adaptive approximation tracking control of a continuum robot with uncertainty disturbances. *IEEE Transactions on Cybernetics*.
- Xu, W., Liu, T., & Li, Y. (2018). Kinematics, dynamics, and control of a cable-driven hyper-redundant manipulator. *IEEE/ASME Transactions on Mechatronics*, 23(4), 1693–1704.
- Xu, K., Mei, W., Yang, Z., Han, L., & Zhu, X. (2014). Design of a hyper-redundant continuum manipulator for intra-cavity tasks. In *2014 IEEE international conference on robotics and biomimetics* (pp. 380–385). IEEE.
- Yan, Y., Jiang, W., Zou, D., Quan, W., Li, H. J., Lei, Y., et al. (2020). Research on mechanism configuration and coordinated control for power distribution network live working robot. *Industrial Robot: The International Journal of Robotics Research and Application*, 47(3), 453–462.
- Yang, Z., Yang, L., Sun, Y., & Chen, X. (2023). Comprehensive kinetostatic modeling and morphology characterization of cable-driven continuum robots for in-situ aero-engine maintenance. *Frontiers of Mechanical Engineering*, 18(3), 40.
- Yao, Y., Huang, Q., Peng, Y., & Oiwa, T. (2011). Hybrid position, posture, force and moment control with impedance characteristics for robot manipulators. In *2011 IEEE international conference on mechatronics and automation* (pp. 2129–2134). IEEE.
- Yao, Z., Wu, H., Yang, Y., Cheng, Y., Pan, H., Zhang, T., et al. (2022). On-line precision control of CFETR multipurpose overload robot using deformation model. *Fusion Engineering and Design*, 174, Article 112967.
- Yeshmukhametov, A., Koganezawa, K., & Yamamoto, Y. (2019). Designing of novel wire-driven continuum robot arm with passive sliding disc mechanism: Forward and inverse kinematics. In *2019 19th international conference on control, automation and systems* (pp. 218–223). IEEE.
- You, P., Liu, Z., & Ma, Z. (2023). Multibody dynamic modeling and analysis of cable-driven snake robot considering clearance and friction based on ALE method. *Mechanics and Machine Theory*, 184, Article 105313.
- Yu, B., & Natarajan, S. (2020). An easy use auxiliary arm: Design and control of a portable continuum manipulator for enhanced dexterity by soft-rigid arms collaboration. In *2020 3rd IEEE international conference on soft robotics* (pp. 164–169). IEEE.
- Zheng, Y., Li, Z., Deng, J., Zou, J., Gu, G., & Zhu, X. (2022). Improving the motion precision of a 24-DoF hyper-redundant robot through kinematic calibration. In *2022 international conference on advanced robotics and mechatronics* (pp. 690–695). IEEE.
- Zheng, Y., Wu, B., Chen, Y., Zeng, L., Gu, G., Zhu, X., et al. (2021). Design and validation of cable-driven hyper-redundant manipulator with a closed-loop puller-follower controller. *Mechatronics*, 78, Article 102605.